

Lévy Adaptive B-spline Regression via Overcomplete Systems

Sewon Park¹, Hee-Seok Oh¹, and Jaeyong Lee¹

¹Department of Statistics, Seoul National University

February 2, 2021

Abstract

The estimation of functions with varying degrees of smoothness is a challenging problem in the nonparametric function estimation. In this paper, we propose the LABS (Lévy Adaptive B-Spline regression) model, an extension of the LARK models, for the estimation of functions with varying degrees of smoothness. LABS model is a LARK with B-spline bases as generating kernels. The B-spline basis consists of piecewise k degree polynomials with $k - 1$ continuous derivatives and can express systematically functions with varying degrees of smoothness. By changing the orders of the B-spline basis, LABS can systematically adapt the smoothness of functions, i.e., jump discontinuities, sharp peaks, etc. Results of simulation studies and real data examples support that this model catches not only smooth areas but also jumps and sharp peaks of functions. The proposed model also has the best performance in almost all examples. Finally, we provide theoretical results that the mean function for the LABS model belongs to the certain Besov spaces based on the orders of the B-spline basis and that the prior of the model has the full support on the Besov spaces.

Key words: Nonparametric Function Estimation; Lévy Random Measure; Besov Space; Reversible Jump Markov Chain Monte Carlo.

1 Introduction

Suppose we observe n pairs of observations, $(x_1, y_1), (x_2, y_2), \dots, (x_n, y_n)$ where

$$y_i = \eta(x_i) + \epsilon_i, \quad \epsilon_i \stackrel{iid}{\sim} \mathcal{N}(0, \sigma^2), \quad i = 1, 2, \dots, n, \quad (1)$$

and η is an unknown real-valued function which maps \mathbb{R} to \mathbb{R} . We wish to estimate the mean function η that may have varying degrees of smoothness including discontinuities. In nonparametric function estimation, we often face smooth curves except for a finite number of jump discontinuities and sharp peaks, which are common in many climate and economic datasets. Heavy rainfalls cause a sudden rise in the water level of a river. The COVID-19 epidemic brought about a sharp drop in unemployment rates. Policymakers' decisions can give rise to abrupt changes. For instance, the United States Congress passed the National Minimum Drinking Age Act in 1984, which has been debated over several decades in the United States, establishing 21 as the minimum legal alcohol purchase age. This act caused a sudden rise in mortality for young Americans around 21. The abrupt changes can provide us with meaningful information on these issues, and it is important to grasp the changes.

There has been much research into the estimation of local smoothness of the functions. The first approach is to minimize the penalized sum of squares based on a locally varying smoothing parameter or penalty function across the whole domain. Pintore et al. (2006), Liu and Guo (2010), and Wang et al. (2013) modeled the smoothing parameter of smoothing spline to vary over the domain. Ruppert and Carroll (2000), Crainiceanu et al. (2007), Krivobokova et al. (2008), and Yang and Hong (2017) suggested the penalized splines based on the local penalty that adapts to spatial heterogeneity in the regression function. The second approach is the adaptive free-knot splines that choose the number and location of the knots from the data. Friedman (1991) and Luo and Wahba (1997) determined a set of knots using stepwise forward/backward knot selection procedures. Zhou and Shen (2001) avoided the problems of stepwise schemes and proposed optimal knot selection schemes introducing the knot relocation step. Smith and Kohn (1996), Denison et al. (1998b), Denison et al. (1998a), and DiMatteo et al. (2001) studied Bayesian estimation of free knot splines using MCMC techniques. The third approach is to use wavelet shrinkage estimators including VisuShrink based on the universal threshold (Donoho and Johnstone; 1994), SureShrink based on Stein's unbiased risk estimator (SURE) function (Donoho and Johnstone; 1995), Bayesian thresholding rules by utilizing a mixture prior (Abramovich

et al.; 1998), and empirical Bayes methods for level-dependent threshold selection (Johnstone and Silverman; 2005). The fourth approach is to detect jump discontinuities in the regression curve. Koo (1997), Lee (2002), and Yang and Song (2014) dealt with the estimation of discontinuous function using B-spline basis functions. Qiu and Yandell (1998), Qiu (2003), Gijbels et al. (2007), and Xia and Qiu (2015) identified jumps based on local polynomial kernel estimation.

In this paper, we consider a function estimation method using overcomplete systems. A subset of the vectors $\{\phi\}_{j \in J}$ of Banach space \mathcal{F} is called a *complete system* if

$$\|\eta - \sum_{j \in J} \beta_j \phi_j\| < \epsilon, \quad \forall \eta \in \mathcal{F}, \forall \epsilon > 0,$$

where $\beta_j \in \mathbb{R}$ and $J \in \mathbb{N} \cup \infty$. Such a complete system is *overcomplete* if removal of a vector ϕ_j from the system does not alter the completeness. In other words, an overcomplete system is constructed by adding basis functions to a complete basis (Lewicki and Sejnowski; 2000). Coefficients β_j in the expansion of η with an overcomplete system are not unique owing to the redundancy intrinsic in the overcomplete system. The non-uniqueness property can provide more parsimonious representations than those with a complete system (Simoncelli et al.; 1992).

The Lévy Adaptive Regression Kernels (LARK) model, first proposed by Tu (2006), is a Bayesian regression model utilizing overcomplete systems with Lévy process priors. Tu (2006) showed the LARK model had sparse representations for η from an overcomplete system and improvements in nonparametric function estimation. Pillai et al. (2007) found out the relationship between the LARK model and a reproducing kernel Hilbert space (RKHS), and Pillai (2008) proved the posterior consistency of the LARK model. Ouyang et al. (2008) extended the LARK method to the classification problems. Chu et al. (2009) used continuous wavelets as the elements of an overcomplete system. Wolpert et al. (2011) obtained sufficient conditions for LARK models to lie in the some Besov space or Sobolev space. Lee et al. (2020) devised an extended LARK model with multiple kernels instead of only one type kernel.

In this paper, we develop a fully Bayesian approach with B-spline basis functions as the elements of an overcomplete system and call it the Lévy Adaptive B-Spline regression (LABS). Our main contributions of this work can be summarized as follows.

1. The LABS model can systematically represent the smoothness of functions varying locally by changing the orders of the B-spline basis. The form of a B-spline basis depends on

the locations of knots and can be symmetrical or asymmetrical. The varying degree of B-spline basis enables the LABS model to adapt to the smoothness of functions.

2. We investigate two theoretical properties of the LABS model. First, the mean function of the LABS model exists in certain Besov spaces based on the types of degrees of B-spline basis. Second, the prior of the LABS model has full support on some Besov spaces. Thus, the proposed LABS model extends the range of smoothness classes of the mean function.
3. We provide empirical results demonstrating that our model performs well in the spatially inhomogeneous functions such as the functions with both jump discontinuities, sharp peaks, and smooth parts. The LABS model achieved the best results in almost every experiments compared to the popular nonparametric function estimation methods. In particular, the LABS model showed remarkable performance in estimating functions with jump discontinuities and outperformed other competing models.

The rest of the paper is organized as follows. In section 2, we introduce the Lévy Adaptive Regression Kernels and discuss its properties. In section 3, we propose the LABS model and present an equivalent model with latent variables that make the posterior computation tractable. We present three theorems that the function spaces for the proposed model depend upon the degree of B-spline basis and that the prior has large support in some function spaces. We describe the detailed algorithm of posterior sampling using reversible jump Markov chain Monte Carlo in section 4. In section 5, the LABS model is compared with other methods in two simulation studies and in section 6 three real-world data sets are analysed using the LABS model. In the last section, we discuss some improvements and possible extensions of the proposed model.

2 Lévy adaptive regression kernels

In this section, we give a brief introduction to the LARK model. Let Ω be a complete separable metric space, and ν be a positive measure on $\mathbb{R} \times \Omega$ with $\nu(\{0\}, \Omega) = 0$ satisfying L_1 integrability condition,

$$\int \int_{\mathbb{R} \times A} (1 \wedge |\beta|) \nu(d\beta, d\omega) < \infty, \quad (2)$$

for each compact set $A \subset \Omega$. The Lévy random measure L with Lévy measure ν is defined as

$$L(d\omega) = \int_{\mathbb{R}} \beta N(d\beta, d\omega),$$

where N is a Poisson random measure with intensity measure ν . We denote $L \sim \text{Lévy}(\nu)$. For any $t \in \mathbb{R}$, the characteristic function of $L(A)$ is

$$\mathbb{E} \left[e^{itL(A)} \right] = \exp \left\{ \int \int_{\mathbb{R} \times A} (e^{it\beta} - 1) \nu(d\beta, d\omega) \right\}, \quad \text{for all } A \subset \Omega. \quad (3)$$

Let $g(x, \omega)$ be a real-valued function defined on $\mathcal{X} \times \Omega$ where \mathcal{X} is another set. By integrating g with respect to a Lévy random measure L , we define a real-valued function on \mathcal{X} :

$$\eta(x) \equiv L[g(x)] = \int_{\Omega} g(x, \omega) L(d\omega) = \int_{\Omega} \int_{\mathbb{R}} g(x, \omega) \beta N(d\beta, d\omega), \quad \forall x \in \mathcal{X}. \quad (4)$$

We call g a *generating function* of η .

When $\nu(\mathbb{R} \times \Omega) = M$ is finite, a Lévy random measure can be represented as $L(d\omega) = \sum_{j \leq J} \beta_j \delta_{\omega_j}$, where J has a Poisson distribution with mean $M > 0$ and $\{(\beta_j, \omega_j)\} \stackrel{iid}{\sim} \pi(d\beta_j, d\omega_j) := \nu/M, j = 1, 2, \dots, J$. In this case, equation (4) can be expressed as

$$\eta(x) = \sum_{j=1}^J g(x, \omega_j) \beta_j, \quad (5)$$

where $\{(\beta_j, \omega_j)\}$ is the random set of finite support points of a Poisson random measure. If g is bounded, L_1 integrability condition (2) implies the existence of (4) for all x . See Lee et al. (2020).

If a Lévy measure satisfying (2) is infinite, the number of the support points of $N(\mathbb{R}, \Omega)$ is infinite almost surely. Tu (2006) proved that the truncated Lévy random field $L_{\epsilon}[g]$ converges in distribution to $L[g]$ as $\epsilon \rightarrow 0$, where

$$L_{\epsilon}[g] = \int \int_{[-\epsilon, \epsilon]^c \times \Omega} g(x, \omega) \beta N(d\beta, d\omega) = \int \int_{\mathbb{R} \times \Omega} g(x, \omega) \beta N_{\epsilon}(d\beta, d\omega),$$

and N_{ϵ} is a Poisson measure on \mathbb{R} with mean measure

$$\nu_{\epsilon}(d\beta, d\omega) := \nu(d\beta, d\omega) I_{|\beta| > \epsilon}.$$

This truncation often used as an approximation of the posterior. For posterior computation methods for the Poisson random measure without truncation, see Lee (2007) and Lee and Kim (2004).

Together with data generating mechanism (1), the LARK model is defined as follows:

$$\mathbb{E}[Y|L, \theta] = \eta(x) \equiv \int_{\Omega} g(x, \omega) L(d\omega)$$

$$L|\theta \sim \text{Lévy}(\nu)$$

$$\theta \sim \pi_{\theta}(d\theta),$$

where Lèvy(ν) denotes the Lèvy process which has the characteristic function and ν is a Lèvy measure satisfying (2). Tu (2006) used gamma, symmetric gamma, and symmetric α -stable (SaS) ($0 < \alpha < 2$) Lèvy random fields. The conditional distribution for Y has a hyperparameter θ and π_θ denotes the prior distribution of θ . The generating function $g(x, \omega)$ is used as elements of an overcomplete system. Tu (2006) and Lee et al. (2020) used the Gaussian kernel, the Laplace kernel, and Haar wavelet as generating functions:

- Haar kernel: $g(x, \omega) := I(|\frac{x-\chi}{\lambda}| \leq 1)$
- Gaussian kernel: $g(x, \omega) = \exp\left\{-\frac{(x-\chi)^2}{2\lambda^2}\right\}$
- Laplacian Kernel: $g(x, \omega) = \exp\left\{-\frac{|x-\chi|}{\lambda}\right\}$

with $\omega := (\chi, \lambda) \in \mathbb{R} \times \mathbb{R}^+ := \Omega$. All of the above generating functions are bounded.

This LARK model can be represented in a hierarchical structure as follows:

$$\begin{aligned}
 Y_i | \eta(\mathbf{x}_i) &\stackrel{i.i.d}{\sim} \mathcal{N}(\eta(\mathbf{x}_i), \sigma^2) \\
 \eta(\mathbf{x}_i) &= \sum_{j=1}^J g(\mathbf{x}_i, \boldsymbol{\omega}_j) \beta_j \\
 J | \epsilon &\sim \text{Pois}(\nu_\epsilon(\mathbb{R}, \Omega)) \\
 (\beta_j, \boldsymbol{\omega}_j) | J, \epsilon &\stackrel{i.i.d}{\sim} \pi(d\beta_j, d\boldsymbol{\omega}_j) := \frac{\nu_\epsilon(d\beta_j, d\boldsymbol{\omega}_j)}{\nu_\epsilon(\mathbb{R}, \Omega)}
 \end{aligned}$$

for $j = 1, \dots, J$. J is the random number that is stochastically determined by Lèvy random measure, $(\beta_1, \dots, \beta_J)$ is the unknown coefficients of a mean function and $(\boldsymbol{\omega}_1, \dots, \boldsymbol{\omega}_J)$ is the parameters of the generating functions. To obtain samples from the posterior distribution under the LARK model, the reversible jump Markov chain Monte Carlo (RJMCMC) proposed by Green (1995) is used because some parameters have varying dimensions.

The LARK model stochastically extracts features and finds a compact representation for $\eta(\cdot)$ based on an overcomplete system. That is, it enables functions to be represented by the small number of elements from an overcomplete system. However, both the LARK model and most methods for function estimation use only one type of kernel or basis and can find out the restricted smoothness of the target function. These models cannot afford to capture all parts of the function with various degrees of smoothness. For example, we consider a noisy modified Heavisine function sampled at $n = 512$ equally spaced points on $[0, 1]$ in Figure 1. The data

contains both smooth and non-smooth regions such as peaks and jumps. As shown in panel (a) of Figure 1, it is difficult for the LARK model with a finite Lévy measure using Gaussian kernel to estimate jump parts of the data. We, therefore, propose a new model which can adapt the smoothness of function systematically by using a variety of B-spline bases as the generating elements of an overcomplete system.

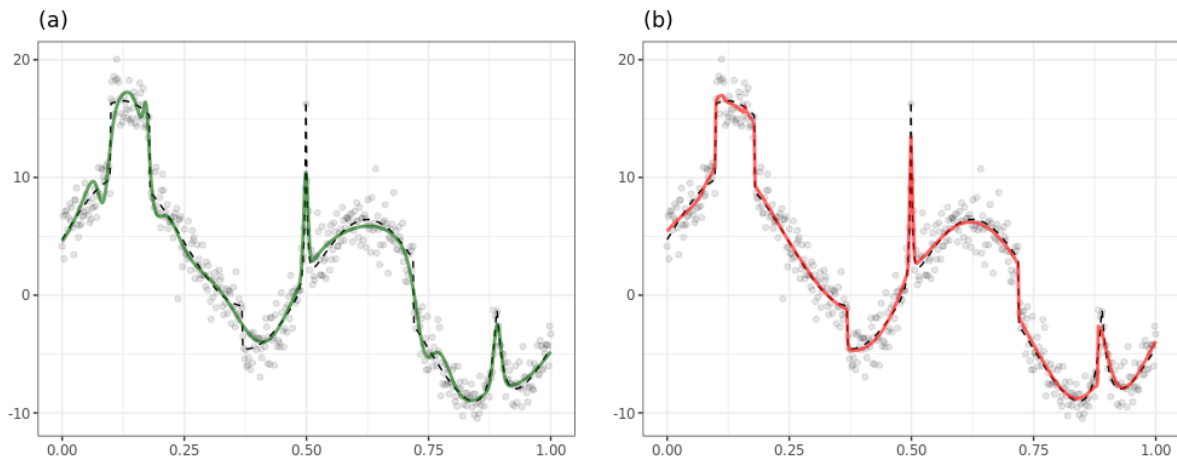


Figure 1: Comparison of curve fitting functions with (a) LARK, and (b) LABS model for the modified heavisine dataset. The solid lines are estimated functions and the dashed line represents the true function.

3 Lévy adaptive B-spline regression

We consider a general type of basis function as the generating elements of an overcomplete system instead of specific kernel functions such as Haar, Laplacian, and Gaussian. The LABS model uses B-spline basis functions which can all systematically express jumps, sharp peaks, and smooth parts of the function.

3.1 B-spline Basis

The B-spline basis function consists of piecewise k degree polynomials with $k - 1$ continuous derivatives. In general, the B-spline basis of degree k can be derived utilizing the Cox-de Boor

recursion formula:

$$B_{0,i}^*(x) := \begin{cases} 1 & \text{if } t_i \leq x < t_{i+1} \\ 0 & \text{otherwise} \end{cases} \quad (6)$$

$$B_{k,i}^*(x) := \frac{x - t_i}{t_{i+k} - t_i} B_{k-1,i}^*(x) + \frac{t_{i+k+1} - x}{t_{i+k+1} - t_{i+1}} B_{k-1,i+1}^*(x),$$

where t_i are called knots which must be in non-descending order $t_i \leq t_{i+1}$ (De Boor; 1972), (Cox; 1972). The B-spline basis of degree k , $B_{k,i}^*(x)$ then needs $(k + 2)$ knots, (t_i, \dots, t_{i+k+1}) . For convenience of notation, we redefine the B-spline basis of degree k with a knot sequence $\boldsymbol{\xi}_k := (\xi_{k,1}, \dots, \xi_{k,k+2})$ as follows.

$$B_0(x; \boldsymbol{\xi}_0) := \begin{cases} 1 & \text{if } \xi_{0,1} \leq x < \xi_{0,2} \\ 0 & \text{otherwise} \end{cases} \quad (7)$$

$$B_k(x; \boldsymbol{\xi}_k) := \frac{x - \xi_{k,1}}{\xi_{k,(k+1)} - \xi_{k,1}} B_{k-1}(x; \boldsymbol{\xi}_k^*) + \frac{\xi_{k,(k+2)} - x}{\xi_{k,(k+2)} - \xi_{k,2}} B_{k-1}(x; \boldsymbol{\xi}_k^{**}),$$

where $\boldsymbol{\xi}_k^* := (\xi_{k,1}, \xi_{k,2}, \dots, \xi_{k,(k+1)})$ and $\boldsymbol{\xi}_k^{**} := (\xi_{k,2}, \xi_{k,3}, \dots, \xi_{k,(k+2)})$.

The B-spline basis functions can have a variety of shapes and smoothness determined by knot locations and the degree of it. For example, a B-spline basis function can be a piecewise constant ($k = 0$), linear ($k = 1$), quadratic ($k = 2$), and cubic ($k = 3$) functions. Furthermore, the B-spline basis with equally spaced knots has the symmetric form. These bases are called a Uniform B-splines. Examples of the B-spline basis functions of different degrees with equally spaced knots are shown in Figure 2.

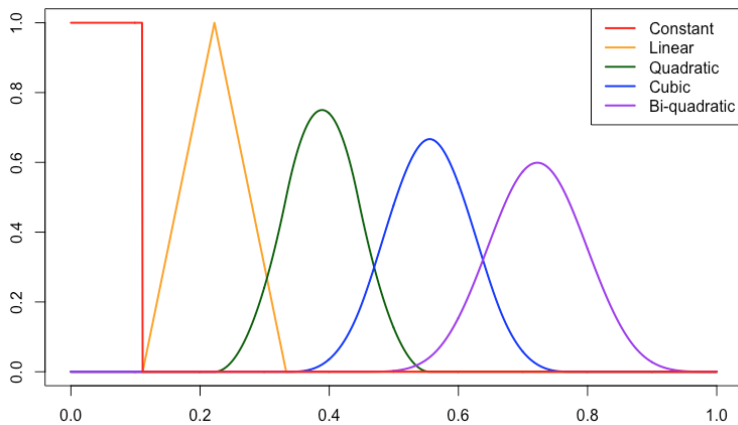


Figure 2: Different shapes of the B-spline basis function by increasing the degree k

3.2 Model Specification

The LARK model with one type of kernel can not estimate well functions with both continuous and discontinuous parts. To improve this, we consider various a B-spline basis functions simultaneously for estimating all parts of the unknown function. The new model uses B-spline basis to systematically generate an overcomplete system with varying degrees of smoothness. For example, the B-spline basis functions of degrees 0, 1 and 2 or more are for jumps, sharp peaks and smooth parts of the function, respectively.

We consider the mean function can be expressed as a random finite sum:

$$\eta(x) = \sum_{k \in S} \sum_{1 \leq l \leq J_k} B_k(x; \boldsymbol{\xi}_{k,l}) \beta_{k,l}, \quad (8)$$

where S denotes the subset of degree numbers of B-spline basis and $B_k(x; \boldsymbol{\xi}_k)$ is a B-spline basis of degree k with knots, $\boldsymbol{\xi}_k \in \mathcal{X}^{(k+2)} := \Omega$. Generating functions of the LARK model are replaced by the B-spline basis functions. J_k has a Poisson distribution with $M_k > 0$ and $\{(\beta_{k,l}, \boldsymbol{\xi}_{k,l})\} \stackrel{iid}{\sim} \pi_k(d\beta_k, d\boldsymbol{\xi}_k) := \nu_k(d\beta_k, d\boldsymbol{\xi}_k) / \nu_k(\mathbb{R} \times \Omega)$. In this paper, we assume

$$\pi_k(d\beta_k, d\boldsymbol{\xi}_k) = \mathcal{N}(\beta_k; 0, \phi_k^2) d\beta_k \cdot \mathcal{U}(\boldsymbol{\xi}_k; \mathcal{X}^{(k+2)}) d\boldsymbol{\xi}_k.$$

The mean function can be also defined as

$$\eta(x) \equiv \sum_{k \in S} \int_{\Omega} B_k(x; \boldsymbol{\xi}_k) L_k(d\boldsymbol{\xi}_k). \quad (9)$$

The stochastic integral representation of the mean function is determined by

$$L_k \sim \text{Lévy}(\nu_k(d\beta_k, d\boldsymbol{\xi}_k)), \quad \forall k \in S,$$

where $\nu_k(d\beta_k, d\boldsymbol{\xi}_k)$ is a finite Lévy measure satisfying $M_k \equiv \nu_k(\mathbb{R} \times \Omega) < \infty$. Although the Lévy measure ν_k satisfying (2) may be infinite, the Poisson integrals and sums above are well defined for all bounded measurable compactly-supported $B_k(\cdot, \cdot)$ for which for all $k \in S$,

$$\int \int_{\mathbb{R} \times \Omega} (1 \wedge |\beta_k B_k(\cdot; \boldsymbol{\xi}_k)|) \nu_k(d\beta_k, d\boldsymbol{\xi}_k) < \infty. \quad (10)$$

In this paper, we consider only finite Lévy measures in the proposed model. In other words, we restrict our attention to the Lévy measure of a compound Poisson process. The new model is more complex than the LARK model with one kernel and expected to give a more accurate

estimate of the regression function. It can estimate a mean function having both smooth and peak shapes. The proposed model can write in hierarchical form as

$$\begin{aligned}
Y_i|x_i &\stackrel{iid}{\sim} \mathcal{N}(\eta(x_i), \sigma^2), \quad i = 1, 2, \dots, n, \\
\eta(x) &= \beta_0 + \sum_{k \in S} \sum_{1 \leq l \leq J_k} B_k(x; \boldsymbol{\xi}_{k,l}) \beta_{k,l}, \\
\sigma^2 &\sim \text{IG}\left(\frac{r}{2}, \frac{rR}{2}\right), \\
J_k &\sim \text{Poi}(M_k), \\
M_k &\sim \text{Ga}(a_{\gamma_k}, b_{\gamma_k}), \\
\beta_{k,l} &\stackrel{iid}{\sim} \mathcal{N}(0, \phi_k^2), \quad l = 1, 2, \dots, J_k, \\
\boldsymbol{\xi}_{k,l} &\stackrel{iid}{\sim} \mathcal{U}(\mathcal{X}^{(k+2)}), \quad l = 1, 2, \dots, J_k,
\end{aligned} \tag{11}$$

for $k \in S$. We set $\beta_0 = \bar{Y}$ and $\phi_k = 0.5 \times (\max_i \{Y_i\} - \min_i \{Y_i\})$.

3.3 Support of LABS model

In this section, we present three theorems on the support of the LABS model. We first define the modulus of smoothness and Besov spaces.

Definition 1 *Let $0 < p \leq \infty$ and $h > 0$. For $f \in L^p(\mathcal{X})$, the r th order modulus of smoothness of f is defined by*

$$\omega_r(f, t)_p := \sup_{h \leq t} \|\Delta_h^r f\|_p,$$

where $\Delta_h^r f(x) = \sum_{k=0}^r \binom{r}{k} (-1)^{r-k} f(x + kh)$ for $x \in \mathcal{X}$ and $x + kh \in \mathcal{X}$.

If $r = 1$, $\omega_1(f, t)_p$ is the modulus of continuity. There exist equivalent definitions in defining Besov spaces. We follow DeVore and Lorentz (1993)[2.10, page 54].

Definition 2 *Let $\alpha > 0$ be given and let r be the smallest integer such that $r > \alpha$. For $0 < p, q < \infty$, the Besov space $\mathbb{B}_{p,q}^\alpha$ is the collection of all functions $f \in L_p(\mathcal{X})$ such that*

$$|f|_{\mathbb{B}_{p,q}^\alpha} = \left(\int_0^\infty [t^{-\alpha} \omega_r(f, t)_p]^q \frac{dt}{t} \right)^{1/q}$$

is finite. The norm on $\mathbb{B}_{p,q}^\alpha$ is defined as

$$\|f\|_{\mathbb{B}_{p,q}^\alpha} = \|f\|_p + |f|_{\mathbb{B}_{p,q}^\alpha}.$$

The Besov space is a general function space depending on the smoothness of functions in $L_p(\mathcal{X})$ and especially can allow smoothness of spatially inhomogeneous functions, including spikes and jumps. The Besov space has three parameters, α , p , and q , where α is the degree of smoothness, p represents that $L_p(\Omega)$ is the function space where smoothness is measured, and q is a parameter for a finer tuning on the degree of smoothness.

Theorem 1 *For fixed $k \in S$ and $\xi_k \in \mathcal{X}^{(k+2)}$, the B-spline basis $B_k(x; \xi_k)$ falls in $\mathbb{B}_{p,q}^\alpha(\mathcal{X})$ for all $1 \leq p, q < \infty$ and $\alpha < k + 1/p$.*

The proof is given in Appendix A. For instance, the B-spline basis with degree 0 satisfies $B_k(\cdot, \xi_k) \in \mathbb{B}_{p,q}^\alpha$ for $\alpha < 1/p$, the B-spline basis with degree 1 is in $\mathbb{B}_{p,q}^\alpha$ for $1 + 1/p$ and the B-spline basis with degree 2 falls in $\mathbb{B}_{p,q}^s$ for $2 + 1/p$.

The following theorem describes the mean function of the LABS model, η , is in a Besov space with smoothness corresponding to degrees of B-spline bases used in the LABS model. The proof of the theorem closely follows that of Wolpert et al. (2011). The proof of Theorem 2 is given in Appendix A.

Theorem 2 *Suppose \mathcal{X} is a compact subset of \mathbb{R} . Let ν_k be a Lévy measure on $\mathbb{R} \times \mathcal{X}^{(k+2)}$ that satisfies the following integrability condition,*

$$\int \int_{\mathbb{R} \times \mathcal{X}^{(k+2)}} (1 \wedge |\beta_k|) \nu_k(d\beta_k, d\xi_k) < \infty. \quad (12)$$

and $L_k \sim \text{Lévy}(\nu_k)$ for all $k \in S$. Define the mean function of the LABS model, $\eta(\cdot) = \sum_{k \in S} \int_{\mathcal{X}^{(k+2)}} B_k(x; \xi_k) L_k(d\xi_k)$ on \mathcal{X} where $B_k(x; \xi_k)$ satisfies (12) for each fixed $x \in \mathcal{X}$. Then, η has the convergent series

$$\eta(x) = \sum_{k \in S} \sum_l B_k(x; \xi_{k,l}) \beta_{k,l} \quad (13)$$

where S is a finite set including degree numbers of B-spline basis. Furthermore, η lies in the Besov space $\mathbb{B}_{p,q}^\alpha(\mathcal{X})$ with $\alpha < \min(S) + \frac{1}{p}$ almost surely.

For example, if a zero element is included in S then the mean function of the LABS, η falls in $\mathbb{B}_{p,q}^\alpha$ with $\alpha < \frac{1}{p}$ almost surely, which consists of functions no longer continuous. If $S = \{3, 5, 8\}$, then, η belongs to $\mathbb{B}_{p,q}^\alpha$ with $\alpha < 3 + \frac{1}{p}$ almost surely. Moreover, it is highly possible that the function spaces for the LABS model may be larger than those of the LARK model using one type of kernel function. Specifically, the mean function for the LABS model with $S = \{0, 1\}$ falls

in $\mathbb{B}_{p,p}^\alpha$ with $\alpha < \frac{1}{p}$ almost surely. If that of the LARK model using only one Laplacian kernel falls in $\mathbb{B}_{p,p}^\alpha$ with $\alpha < 1 + \frac{1}{p}$, then the function spaces of the LABS model with given $\alpha < \frac{1}{p}$ are larger than those of the LARK model for the range of smoothness parameter, $\frac{1}{p} < \alpha < 1 + \frac{1}{p}$ by the properties of the Besov space.

The next theorem shows that the prior distribution of our LABS model has sufficiently large support on the Besov space $\mathbb{B}_{p,q}^\alpha$ with $1 \leq p, q < \infty$ and $\alpha > 0$. For $\eta_0 \in \mathbb{B}_{p,q}^\alpha(\mathcal{X})$, denote the ball around η_0 of radius δ ,

$$\bar{b}_\delta(\eta_0) = \{\eta : \|\eta - \eta_0\|_p < \delta\}$$

where $\|\cdot\|_p$ is a L_p norm. The proof of Theorem 3 is given in Appendix A.

Theorem 3 *Let \mathcal{X} be a bounded domain in \mathbb{R} . Let ν_k be a finite measure on $\mathbb{R} \times \mathcal{X}^{(k+2)}$ and $L_k \sim \text{Levy}(\nu_k)$ for all $k \in S$. Suppose η has a prior Π for the LABS model (11). Then, $\Pi(\bar{b}_\delta(\eta_0)) > 0$ for every $\eta_0 \in \mathbb{B}_{p,q}^\alpha(\mathcal{X})$ and all $\delta > 0$.*

4 Algorithm

Based on the prior specifications and the likelihood function, the joint posterior distribution of the LABS model (11) is

$$\begin{aligned} [\boldsymbol{\beta}, \boldsymbol{\xi}, \mathbf{J}, \mathbf{M}, \sigma^2 | \mathbf{Y}] &\propto [\mathbf{Y} | \eta, \sigma^2] \times [\boldsymbol{\beta}, \boldsymbol{\xi} | \mathbf{J}] \times [\mathbf{J} | \mathbf{M}] \times [\mathbf{M}] \times [\sigma^2] \\ &\propto \left[(\sigma^2)^{-n/2} \exp \left\{ -\frac{1}{2\sigma^2} \sum_{i=1}^n (Y_i - \beta_0 - \sum_{k \in S} \sum_{l=1}^{J_k} B_k(x_i; \boldsymbol{\xi}_{k,l}) \beta_{k,l})^2 \right\} \right] \\ &\times \prod_{k \in S} \left[\exp \left\{ -\frac{1}{2\sigma_k^2} \sum_{l=1}^{J_k} \beta_{k,l}^2 \right\} \right] \times \prod_{k \in S} \left[\frac{1}{|\mathcal{X}^{(k+2)}|^{J_k}} \prod_{l=1}^{J_k} I(\boldsymbol{\xi}_{k,l} \in \mathcal{X}^{(k+2)}) \right] \\ &\times \prod_{k \in S} \left[\frac{M_k^{J_k}}{J_k!} \exp\{-M_k\} \right] \times \prod_{k \in S} \left[M_k^{a_{\gamma_k}-1} \exp\{-b_{\gamma_k} M_k\} \right] \\ &\times \left[(\sigma^2)^{-\frac{r}{2}+1} \exp \left\{ -\frac{rR}{2\sigma^2} \right\} \right]. \end{aligned} \quad (14)$$

The parameters $\boldsymbol{\beta}$ and $\boldsymbol{\xi}$ of the LABS model have varying dimensions as J_k is a random variable. We use the Reversible Jump Markov Chain Monte Carlo (RJMCMC) algorithm (Green; 1995) for the posterior computation.

We consider three transitions in the generation of posterior samples: (a) the addition of basis functions and coefficients; (b) the deletion of basis functions and coefficients; (c) the relocation

of knots which affects the shape of basis functions and coefficients. Note that in step (c) the numbers of basis functions and coefficients do not change. We call such move types birth step, death step, and relocation step, respectively. A type of move is determined with probabilities p_b , p_d and p_w with $p_b + p_d + p_w = 1$, where p_b , p_d and p_w are probabilities of choosing the birth, death, and relocation steps, respectively.

Let us denote $\theta_{k,l} = (\beta_{k,l}, \boldsymbol{\xi}_{k,l})$ by an element of $\boldsymbol{\theta}_k = \{\theta_{k,1}, \theta_{k,2}, \dots, \theta_{k,j}, \dots, \theta_{k,J_k}\}$, where each $\boldsymbol{\xi}_{k,l}$ has the $(k+2)$ dimensions. In general, the acceptance ratio of the RJMCMC can be expressed as

$$A = \min [1, (\text{likelihood ratio}) \times (\text{prior ratio}) \times (\text{proposal ratio}) \times (\text{Jacobian})].$$

In our problem the acceptance ratio for each move types is given by

$$A = \min \left[1, \frac{L(\mathbf{Y}|\boldsymbol{\theta}'_k, J'_k) \Pi(\boldsymbol{\theta}'_k|J'_k) \Pi(J'_k) q(\boldsymbol{\theta}_k|\boldsymbol{\theta}'_k)}{L(\mathbf{Y}|\boldsymbol{\theta}_k, J_k) \Pi(\boldsymbol{\theta}_k|J_k) \Pi(J_k) q(\boldsymbol{\theta}'_k|\boldsymbol{\theta}_k)} \right], \quad (15)$$

where $\boldsymbol{\theta}_k$ and J_k refer to the current model parameters and the number of basis functions in the current state, $\boldsymbol{\theta}'_k$ and J'_k denote the proposed model parameters and the number of basis functions of the new state. Here, the Jacobian is 1 in all move types. $q(\boldsymbol{\theta}'_k|\boldsymbol{\theta}_k)$ is the jump proposal distribution that proposes a new state $\boldsymbol{\theta}'_k$ given a current state $\boldsymbol{\theta}_k$. Specifically, we choose the following jump proposal density proposed by Lee et al. (2020) for each move steps:

$$\begin{aligned} q_b(\boldsymbol{\theta}'_k|\boldsymbol{\theta}_k) &= p_b \times b(\theta_{k,J_{k+1}}) \times \frac{1}{J_k + 1}, \\ q_d(\boldsymbol{\theta}'_k|\boldsymbol{\theta}_k) &= p_d \times \frac{1}{J_k}, \\ q_w(\boldsymbol{\theta}'_k|\boldsymbol{\theta}_k) &= p_w \times q(\boldsymbol{\theta}'_{k,r}|\theta_{k,r}), \end{aligned}$$

where $b(\cdot)$ is a candidate distribution which proposes a new element. For death and change steps, a randomly chosen r th element of $\boldsymbol{\theta}_k$ is deleted and rearranged, respectively. The details regarding updating schemes of each move steps are as follows.

- (a) [**Birth step**] Assume that the current model is composed of J_k basis functions. If the birth step is selected, a new basis function $B_{k,J_{k+1}}$ and $\theta_{k,J_{k+1}}$ is accepted with the acceptance ratio

$$\min \left[1, \frac{L(\mathbf{Y}|\boldsymbol{\theta}'_k, J'_k)}{L(\mathbf{Y}|\boldsymbol{\theta}_k, J_k)} \times \frac{\pi(\theta_{k,J_{k+1}}) M_k}{(J_k + 1)} \times \frac{p_d/(J_k + 1)}{(p_b \times b(\theta_{k,J_{k+1}}))/(J_k + 1)} \right].$$

Especially, a coefficient $\beta_{k,J_{k+1}}$ and an ordered knot set $\boldsymbol{\xi}_{k,J_{k+1}}$ are drawn from their generating distributions and added at the end of $(\beta_{k,1}, \dots, \beta_{k,J_k})$ and $(\boldsymbol{\xi}_{k,1}, \dots, \boldsymbol{\xi}_{k,J_k})$. When $J_k = 0$, the birth step must be exceptionally selected until J_k becomes one.

- (b) **[Death step]** If the death step is selected, a r th element, $\theta_{k,r}$ uniformly chosen is removed from the existing set of basis functions, coefficients and ordered knot sets. We can find out the acceptance ratio for a death step similarly. The acceptance ratio is given by

$$\min \left[1, \frac{L(\mathbf{Y}|\boldsymbol{\theta}'_k, J'_k)}{L(\mathbf{Y}|\boldsymbol{\theta}_k, J_k)} \times \frac{J_k}{\pi(\theta_{k,r})M_k} \times \frac{(b(\theta_{k,r}) \times p_b)/J_k}{p_d/J_k} \right].$$

- (c) **[Relocation step]** Unlike the other steps, the relocation step keeps the numbers of basis functions or coefficients or ordered knot sets fixed. Therefore, the updating scheme of this step is a Metropolis-Hastings within Gibbs sampler. If the relocation step is selected, a current location $\theta_{k,r}$ is moved to a new location $\theta'_{k,r}$ generated by proposal distributions with the acceptance ratio (16). Particularly, since knots of basis function must be in non-descending order, $\xi_{k,r,i}$ which is the i th element of an ordered knot set is sequentially replaced with a new knot location $\xi'_{k,r,i}$ generated by $\mathcal{U}(\xi_{k,r,i-1}, \xi_{k,r,i+1})$, $i = 1, \dots, (k+2)$, where $\xi_{k,r,0}$ and $\xi_{k,r,k+1}$ are boundary points of \mathcal{X} . That is, each element of a specific knot set $\boldsymbol{\xi}_{k,r} = (\xi_{k,r,1}, \dots, \xi_{k,r,k+2})$ is moved to new knot locations $\boldsymbol{\xi}'_{k,r} = (\xi'_{k,r,1}, \dots, \xi'_{k,r,k+2})$ in turn. The corresponding acceptance ratio is given by

$$\min \left[1, \frac{L(\mathbf{Y}|\boldsymbol{\theta}'_k, J'_k)}{L(\mathbf{Y}|\boldsymbol{\theta}_k, J_k)} \times \frac{\pi(\theta'_{k,r})}{\pi(\theta_{k,r})} \times \frac{q_w(\theta_{k,r}|\theta'_{k,r})}{q_w(\theta'_{k,r}|\theta_{k,r})} \right]. \quad (16)$$

When using an independent proposal distribution (i.e. $q_w(\theta'_{k,r}|\theta_{k,r}) = \pi(\theta'_{k,r})$), the acceptance ratio can reduce to

$$\min \left[1, \frac{L(\mathbf{Y}|\boldsymbol{\theta}'_k, J'_k)}{L(\mathbf{Y}|\boldsymbol{\theta}_k, J_k)} \right].$$

Finally, $\beta'_{k,r}$ is sampled from its conditional posterior distribution by using the Gibbs sampling.

The posterior samples of σ and M_k can be generated from their conditional posterior distributions. See Appendix C. The pseudo-code for the proposed strategy is given in Algorithm 1.

Algorithm 1 A reversible jump MCMC algorithm for LABS

```
1: procedure LABS( $S$ ) ▷  $S$ : set of degree numbers
2:   Initialize parameters  $\mathbf{J}, \boldsymbol{\beta}, \boldsymbol{\xi}, \mathbf{M}, \sigma^2$  from prior distributions.
3:   for iteration  $i = 1$  to  $N$  do
4:     for  $k = 1$  to  $|S|$  do ▷  $\mathbf{J} := \{\mathbf{J}_1, \dots, \mathbf{J}_k, \dots, \mathbf{J}_{|S|}\}$ 
5:       Update  $(\mathbf{J}_k, \boldsymbol{\beta}_k, \boldsymbol{\xi}_k)$  through a reversible jump MCMC.
6:       Sample  $M_k$  from the full conditional  $\pi(M_k|\text{others})$ . ▷ Gibbs step
7:     end for
8:     Sample  $\sigma^2$  from the full conditional  $\pi(\sigma^2|\boldsymbol{\beta}, \boldsymbol{\xi}, \mathbf{J}, \mathbf{M}, \mathbf{y})$ . ▷ Gibbs step
9:     Store  $i$ th MCMC samples.
10:  end for
11: end procedure
```

5 Simulation Studies

In this section, we evaluate the performance of the LABS model (11) and competing methods on simulated data sets. First, we apply the proposed method to four standard examples: Bumps, Blocks, Doppler and Heavisine test functions introduced by Donoho and Johnstone (1994). Second, we consider three functions that we created ourselves with jumps and peaks to assess the practical performance of the proposed model.

The simulated data sets are generated from equally spaced x 's on $\mathcal{X} = [0, 1]$ with sample sizes $n = 128$ and 512 . Independent normally distributed noises $\mathcal{N}(0, \sigma^2)$ are added to the true function $\eta(\cdot)$. The root signal-to-noise ratio (RSNR) is defined as

$$\text{RSNR} := \sqrt{\frac{\int_{\mathcal{X}} (f(x) - \bar{f})^2 dx}{\sigma^2}},$$

where $\bar{f} := \frac{1}{|\mathcal{X}|} \int_{\mathcal{X}} f(x) dx$ and set at 3, 5 and 10. We also run the LABS model for 200,000 iterations, with the first 100,000 iterations discarded as burn-in and retain every 10th sample. For comparison between the methods, we compute the mean squared errors of all methods using 100 replicate data sets for each test function. The average of the posterior curves is used for the estimate of the test function.

$$\text{MSE} = \frac{1}{n} \sum_{i=1}^n (\eta(x_i) - \hat{\eta}(x_i))^2.$$

5.1 Simulation 1 : DJ test functions

We carry out a simulation study using the benchmark test functions suggested by Donoho and Johnstone (1994) often used in the field of wavelet and nonparametric function estimation. The Donoho and Johnstone test functions consist of four functions called Bumps, Blocks, Doppler and Heavisine. These test functions are composed of various shapes such as sharp peaks (Bumps), jump discontinuities (Blocks), oscillating behavior (Doppler) and jumps/peaks in smooth functions (Heavisine) (See Figure 3).

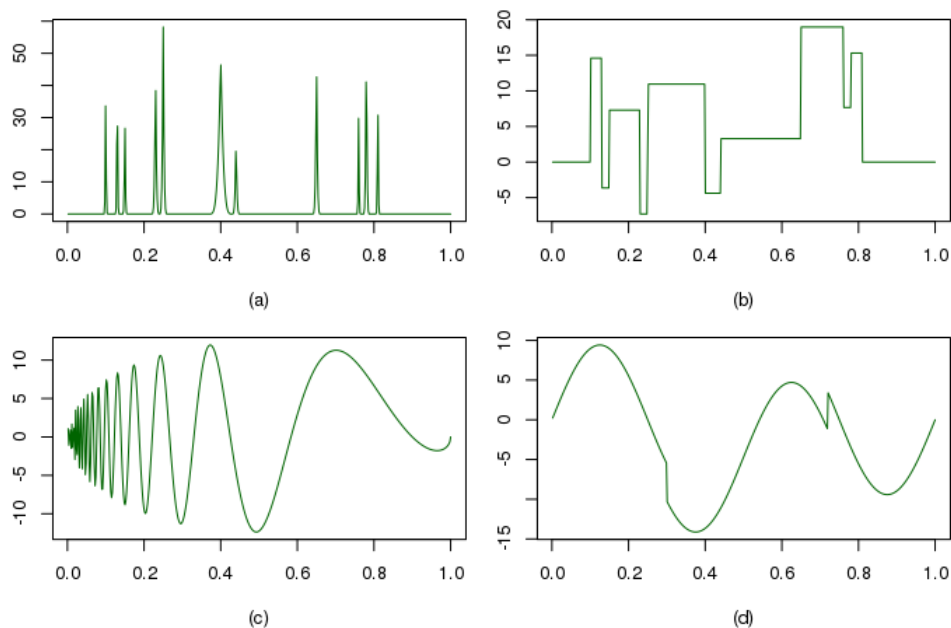


Figure 3: The Donoho and Johnstone test functions: (a) Bumps, (b) Blocks, (c) Doppler and (d) Heavisine

The hyperparameters and types of basis functions displayed in Table 1 were used in (11). For Bumps and Doppler, the parameter r of prior distribution for σ^2 was set to 100 to speed up convergence. We also took account of the combinations of a B-spline basis based on the shapes of test functions.

We compared our model with a variety of methods such as B-spline curve of degree 2 with 50 knots (denoted as BSP-2), Local polynomial regression with automatic smoothing parameter selection (denoted by LOESS), Smoothing spline with smoothing parameter selected by cross-validation (denoted by SS), Nadaraya–Watson kernel regression using the Gaussian kernel

	S	r	R	a_{γ_k}	b_{γ_k}
Bumps	{1}	100	0.01	1	1
Blocks	{0}	0.01	0.01	1	1
Doppler	{1,2}	100	0.01	1	1
Heavisine	{0,2}	0.01	0.01	1	1

Table 1: The values of hyperparameters of proposed model for each test function

with bandwidth h which minimizes CV error (denoted by NWK), Empirical Bayes approach for wavelet shrinkage using a Laplace prior with Daubechies “least asymmetric” (la8) wavelets except for the Blocks example, where it uses the Haar wavelet; Johnstone and Silverman (2005) (denoted by EBW), Gaussian process regression with the Radial basis or Laplacian kernel (denoted by GP-R or GP-L), Bayesian curve fitting using piecewise polynomials with $l = \#1, l_0 = \#2$; Denison et al. (1998b) (denoted by BPP- $\#1$ - $\#2$), Bayesian adaptive spline surfaces with degree $\#$; Francom et al. (2018) (denoted by BASS- $\#$), and Lévy adaptive regression with multiple kernels; Lee et al. (2020) (denoted by LARMuK). These competitive models are implemented in R (R Core Team; 2020) with various packages: LOESS (Wang; 2010), Empirical Bayes thresholding (Silverman et al.; 2005), Gaussian process (Karatzoglou et al.; 2004), Bayesian curve fitting using piecewise polynomials (Feng; 2013), and Bayesian adaptive spline surfaces (Francom and Sanso; 2016).

Both Figure 4 and Figure 5 show that the performance of our model is generally more accurate than other methods. The models in the two figures are selected by better outcomes from simulations. More detailed simulation results can be seen in Appendix B. Figure 4 shows that the LABS model is superior to others regardless of noise levels with $n = 128$. It also has the smallest average mean square errors for all test functions except the Heavisine example with $\text{RSNR} = 3$. Similarly, for sample size $n = 512$, the LABS model comes up with the best performance in Figure 5 except for the Doppler function, where it is competitive. Our model removes high frequencies in the interval $[0, 0.1]$ and produces a smooth curve within the corresponding domain. On the contrary, due to a small number of data points in the Doppler example with $n = 128$, most models yield similar smooth curves in $[0, 0.1]$. As a result, the LABS model has an excellent numerical performance. For Blocks example, LABS, in particular, yields the lowest average and

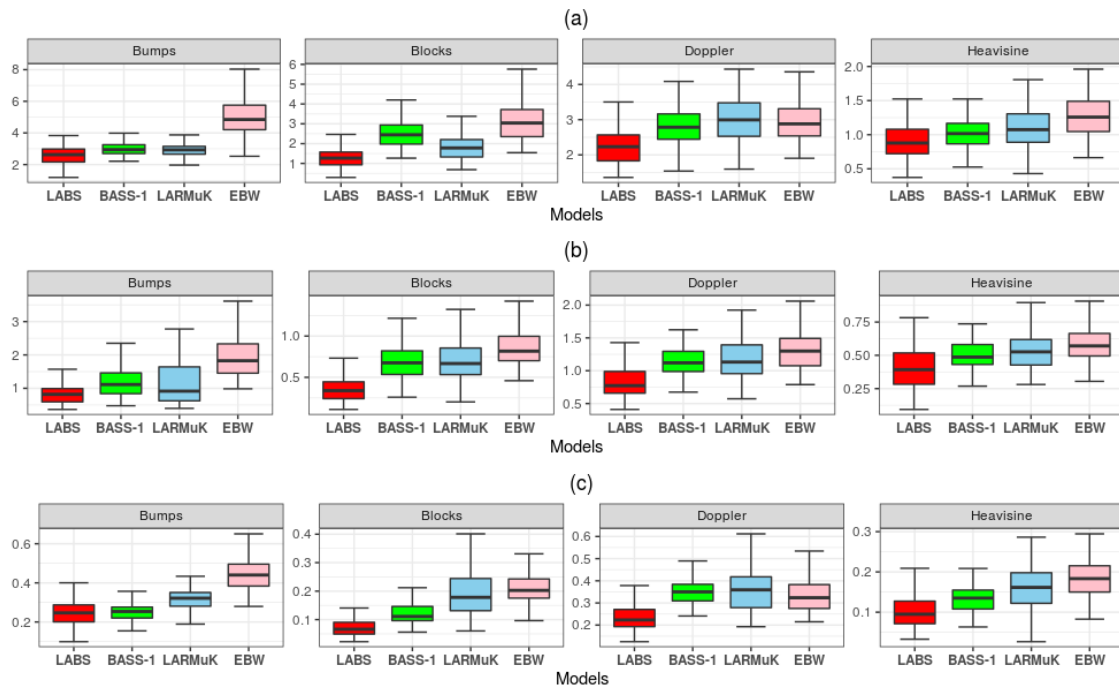


Figure 4: Boxplots of MSEs from the simulation study with $n = 128$ and RSNR = (a) 3, (b) 5 and (c) 10

standard deviation of mean square errors in all scenarios. This suggests that our model has an excellent ability to find jump points. Furthermore, LABS has consistently better performance than B-spline regression using only one basis function for four simulated data sets since its overcomplete systems can be constructed by various combinations of B-spline basis functions. See Appendix B.

5.2 Simulation 2 : Smooth functions with jumps and peaks

Our main interest lies in estimating smooth functions with either discontinuity such as jumps or sharp peaks or both. We design three test functions to assess the practical performance of the proposed method for our concerns. The first and second example is modified by adding some smooth parts, unlike the original version of the Bumps and Blocks of DJ test functions. Each

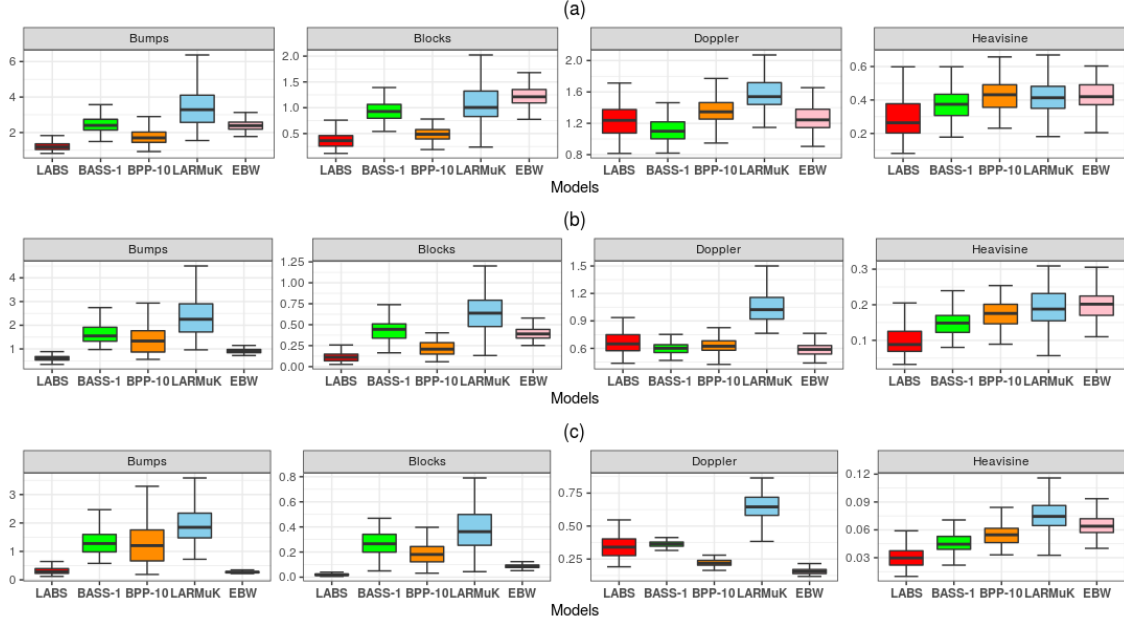


Figure 5: Boxplots of MSEs from the simulation study with $n = 512$ and RSNR = (a) 3, (b) 5 and (c) 10

test functions provided is given by

$$\begin{aligned} \eta_1(x) &= \frac{0.6}{0.92} [4\text{ssgn}(x - 0.1) - 5\text{ssgn}(x - 0.13) + 5\text{ssgn}(x - 0.25) - 4.2\text{ssgn}(x - 0.4) \\ &\quad + 2.1\text{ssgn}(x - 0.44) + 4.3\text{ssgn}(x - 0.65) - 4.2\text{ssgn}(x - 0.81) + 2] + 0.2 + \sin(8\pi x), \\ \eta_2(x) &= [7K_{0.005}(x - 0.1) + 5K_{0.07}(x - 0.25) + 4.2K_{0.03}(x - 0.4) + 4.3K_{0.01}(x - 0.65) \\ &\quad + 5.1K_{0.008}(x - 0.78) + 3.1K_{0.1}(x - 0.9)] + \cos(4\pi x), \end{aligned}$$

where $\text{sgn}(x) = \mathbf{I}_{(0,\infty)}(x) - \mathbf{I}_{(-\infty,0)}(x)$, $\text{ssgn}(x) = 1 + \text{sgn}(x)/2$ and $K_w(x) := (1 + |x/w|)^{-4}$. Finally, we create a sum of jumps, peaks and some smoothness. A formula for a final test function is

$$\begin{aligned} \eta_3(x) &= 6\sin(4\pi x) + 7(1 + \text{sgn}(x - 0.1)/2) - 7(1 + \text{sgn}(x - 0.18)/2) \\ &\quad - 2\text{sgn}(x - 0.37) + 17K_{0.01}(x - 0.5) - 3\text{sgn}(x - 0.72) + 10K_{0.05}(x - 0.89). \end{aligned}$$

They are displayed in Figure 6. We call in turn them modified Blocks, modified Bumps, and modified Heavisine, respectively.

In these experiments, we use two or more types of B-spline basis as elements of overcomplete systems since three functions have different shapes, unlike previous simulation studies. Hyper-

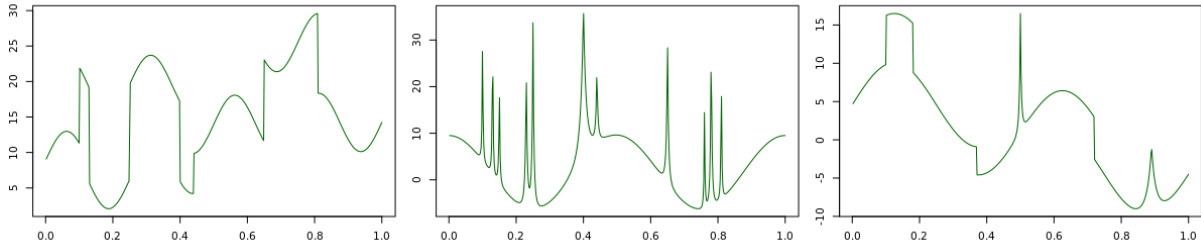


Figure 6: The three test functions used in the second simulation: Modified Blocks (left), Modified Bumps (center) and Modified Heavisine (right)

parameters are similar to the previous ones. All hyperparameters for the prior distributions are summarized in Table 2. This time again, we only compare our model with BPP, BASS, EBW, and LARMuK models which have relatively good performance in some test functions of Simulation 1.

	S	r	R	a_{γ_k}	b_{γ_k}
Modified Blocks	{0,2,3}	0.01	0.01	1	1
Modified Bumps	{1,2}	50	0.01	1	1
Modified Heavisine	{0,1,2,3}	0.01	0.01	5	1

Table 2: Details of hyperparameters of the LABS used in second experiment

Table 3 furnishes that the LABS model has the best outcomes when the sample size is 128, which is difficult to estimate. Furthermore, when $n = 512$, we find out from both Table 4 and Figure 7 that the LABS model performs well in most cases with either the lowest or the second lowest average MSE values across 100 replicates. In particular, the LABS outperforms competitors in modified Blocks, irrespective of the sample size and noise levels as expected. Among all models, the worst performing method is the BASS-2 since it cannot estimate well many jumps or peak points for given test functions. Figure 8 supports that the LABS model has the abilities to overcome the noise and adapt to smooth functions with either discontinuity such as jumps or sharp peaks or both.

Model	Modified Blocks			Modified Bumps			Modified Heavisine		
	RSNR=3	RSNR=5	RSNR=10	RSNR=3	RSNR=5	RSNR=10	RSNR=3	RSNR=5	RSNR=10
EBW	3.781(0.7407)	1.538(0.3854)	0.401(0.0684)	3.921(1.0117)	1.557(0.3191)	0.445(0.1043)	2.548(0.4738)	1.326(0.2793)	0.402(0.095)
BPP-10	2.238(0.6436)	0.951(0.2439)	0.367(0.098)	2.949(0.749)	1.351(0.3244)	0.631(0.2488)	2.06(0.645)	0.824(0.2125)	0.287(0.0907)
BPP-21	2.589(0.4787)	1.336(0.2305)	0.985(0.1714)	3.777(0.9094)	2.586(0.6268)	2.39(0.6003)	2.168(0.3821)	1.228(0.2969)	0.825(0.3458)
BASS-1	2.283(0.5013)	0.76(0.2194)	0.172(0.0424)	2.199(0.5625)	0.858(0.1622)	0.276(0.0483)	2.013(0.5502)	0.737(0.198)	0.178(0.0418)
BASS-2	4.038(0.6519)	2.232(0.371)	1.368(0.168)	9.881(1.1796)	7.944(0.7727)	6.999(0.5772)	3.275(0.3734)	2.276(0.3877)	1.378(0.2871)
LARMuK	2.158(0.5735)	0.97(0.2352)	0.298(0.0929)	2.029(0.7688)	0.822(0.2446)	0.271(0.0944)	1.721(0.4757)	0.713(0.1912)	0.219(0.075)
LABS	1.868(0.5982)	0.691(0.2022)	0.162(0.044)	2.01(0.6006)	0.803(0.1491)	0.248(0.0457)	1.589(0.5081)	0.635(0.1727)	0.172(0.0472)

Table 3: Average of MSEs over 100 replications for three functions of Simulation 2 with $n = 128$. Estimated standard errors of MSEs are shown in parentheses

Model	Modified Blocks			Modified Bumps			Modified Heavisine		
	RSNR=3	RSNR=5	RSNR=10	RSNR=3	RSNR=5	RSNR=10	RSNR=3	RSNR=5	RSNR=10
EBW	1.525(0.228)	0.644(0.1025)	0.171(0.0245)	1.487(0.2056)	0.595(0.0847)	0.171(0.0217)	1.106(0.1523)	0.538(0.0775)	0.153(0.0218)
BPP-10	0.608(0.1362)	0.256(0.055)	0.133(0.0412)	1.2(0.1951)	0.623(0.2658)	0.37(0.2954)	0.602(0.123)	0.237(0.0495)	0.079(0.0183)
BPP-21	0.869(0.1552)	0.424(0.0683)	0.283(0.0479)	1.209(0.3056)	0.937(0.3201)	0.789(0.3442)	0.679(0.1367)	0.275(0.0562)	0.134(0.0338)
BASS-1	0.701(0.1489)	0.296(0.0667)	0.124(0.0455)	0.927(0.147)	0.442(0.0726)	0.197(0.063)	0.561(0.126)	0.246(0.0423)	0.083(0.0166)
BASS-2	4.038(0.6519)	2.232(0.371)	1.368(0.168)	9.881(1.1796)	7.944(0.7727)	6.999(0.5772)	3.275(0.3734)	2.276(0.3877)	1.378(0.2871)
LARMuK	0.775(0.257)	0.416(0.1317)	0.213(0.0841)	1.222(0.4575)	0.805(0.3056)	0.514(0.177)	0.669(0.1749)	0.323(0.0975)	0.14(0.0456)
LABS	0.583(0.1718)	0.234(0.0696)	0.071(0.0325)	0.919(0.1397)	0.46(0.0867)	0.194(0.0443)	0.576(0.146)	0.236(0.0575)	0.078(0.024)

Table 4: Average of MSEs over 100 replications for three functions of Simulation 2 with $n = 512$. Estimated standard errors of MSEs are shown in parentheses

6 Real data applications

We now apply LABS model (11) real-world datasets, including the minimum legal drinking age (MLDA) on mortality rate, the closing bitcoin price index, and the daily maximum value of concentrations of fine particulate matter (PM2.5) in Seoul. All the real data examples exhibit wildly varying patterns that may have jumps or peaks. These fluctuating patterns are expected to further illustrate the features of the LABS model.

In the following applications we set the hyperparameter values of the proposed model, LABS: $a_J = 5$, $b_J = 1$, $r = 0.01$, and $R = 0.01$. In this analysis, we practically choose $S = \{0, 1, 2\}$ because the true curve of real data is unknown and it may have varying smoothness. We run it 200,000 times with a burn-in of 100,000 and thin by 10 to achieve convergence of the MCMC algorithm. Performance comparisons of our model and some rather good methods in the simulated studies are also conducted.

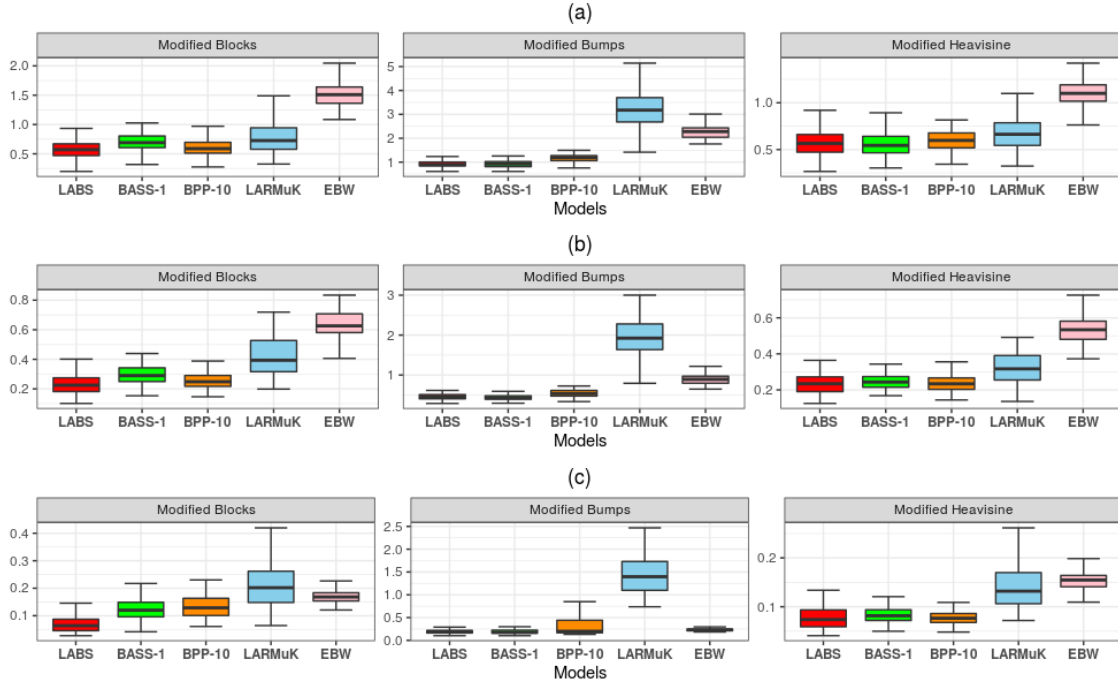


Figure 7: Boxplots of MSEs from the second simulation with $n = 512$ and $\text{RSNR} =$ (a) 3, (b) 5 and (c) 10

6.1 Example 1: Minimum legal drinking age

The Minimum legal drinking age (MLDA) heavily affects youth alcohol consumption which has been a sensitive issue worldwide for policymakers. In the past three decades, there have been many studies on the effect of legal access age to alcohol on death rates. The MLDA dataset collected from Angrist and Pischke (2014) contains death rates, a measure of the total number of deaths per 100,000 young Americans per year.

This data has been widely used to estimate the causal effect of policies on the minimum legal drinking age in the area of Regression Discontinuity Design (RDD). Figure 9 (a) highlights that the MLDA data might represent a piecewise smooth function with a single jump discontinuity at minimum drinking age of 21 referred to as cutoff in the RDD. Specifically, each observation (or point) in Figure 9 corresponds to the death rate from all causes in the monthly interval and the number of all observations is 48.

Using the MLDA data, we estimate unknown functions of death rates via LABS and several competing models including BPP-21, BASS-1, LARMuK, and GP-R. Figure 9 (b) shows that

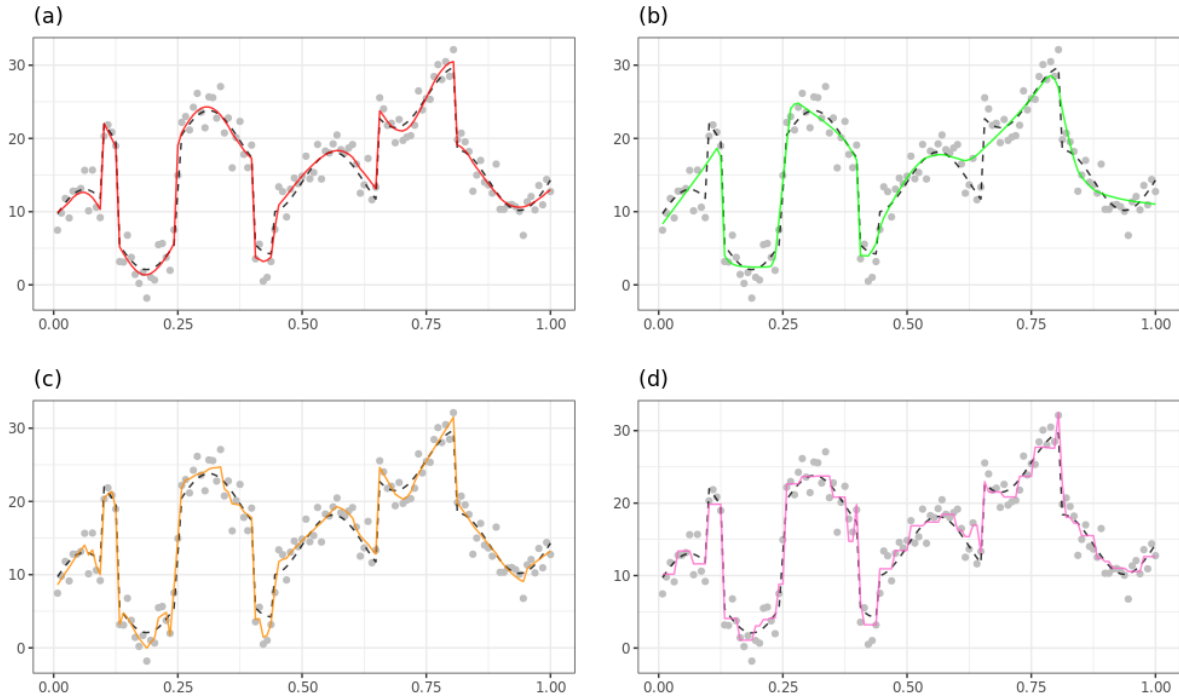


Figure 8: Comparisons of the estimates of a data set generated from the modified Blocks with $n = 128$ and $\text{RSNR} = 3$ using (a) LABS, (b) BASS-1, (c) BPP-10, and (d) EBW. Dashed lines represent true curves, solid lines represent estimates of curve.

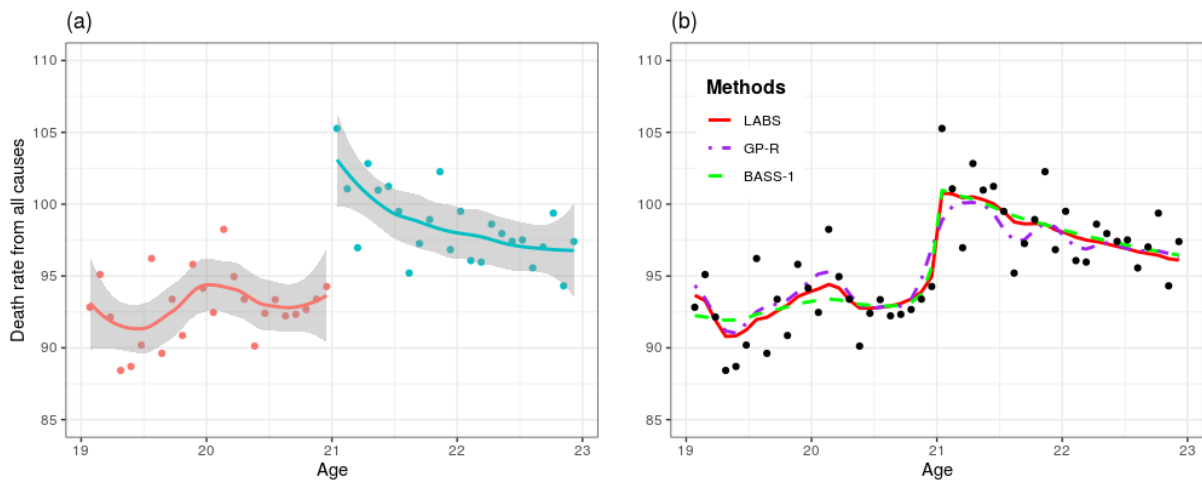


Figure 9: (a) A piecewise curve fitting and (b) comparisons of the fitted posterior mean using BASS-1, GP-R and LABS for Minimum legal drinking age (MLDA) dataset

three posterior mean estimates for an unknown function. The solid curve denotes LABS, the dotted-dashed curve indicates GP-R, and the dashed curve represents BASS-1, respectively.

In Figure 9 (b), both LABS and BASS-1 provide similar posterior curves to the piecewise polynomial regression of Figure 9 (a). The estimated curves of them also have a jump point at 21. While the estimated function of GP-R is smooth, the mean function for the LABS model has both smooth and jump parts. We calculated the mean squared error with 10-folds cross-validation for comparison between methods. The mean and standard deviation values of cross-validation prediction errors are given in Table 5. The smaller CV error rate of LABS implies that LABS has a better performance of estimating a smooth function with discontinuous points than the others.

	LABS	BASS-1	BPP-21	LARMuK	GP-R
Mean	6.5851	6.7884	8.6643	8.35014	7.25693
Standard Deviation	5.1838	4.98241	6.66641	6.45711	5.23563

Table 5: Mean and standard deviation for the error rate of 10-folds cross-validation on MLDA dataset.

6.2 Example 2: Bitcoin prices on Bitstamp

Bitcoin is the best-known cryptocurrency based on Blockchain technology. The demands for bitcoin have increased globally because of offering a higher yield and easy access. The primary characteristic of bitcoin is to enable financial transactions from user to user on the peer-to-peer network configuration without a central bank. Unlimited trading methods and smaller market size than the stock market lead to high volatility in the bitcoin price. We collected a daily bitcoin exchange rate (BTC vs. USD) on Bitstamp from January 1, 2017, to December 31, 2018. Bitcoin data (sourced from <http://www.bitcoincharts.com>) has 730 observations and 8 variables: date, open price (in USD), high price, low price, closing price, volume in bitcoin, volume in currency, and weighted bitcoin price.

We also added LOESS (locally estimated scatterplot smoothing) regression line to a scatter plot of a daily closing price in Figure 10. The dataset shows locally strong upward and downward movements. We apply LABS and other models to estimate the curve of daily bitcoin

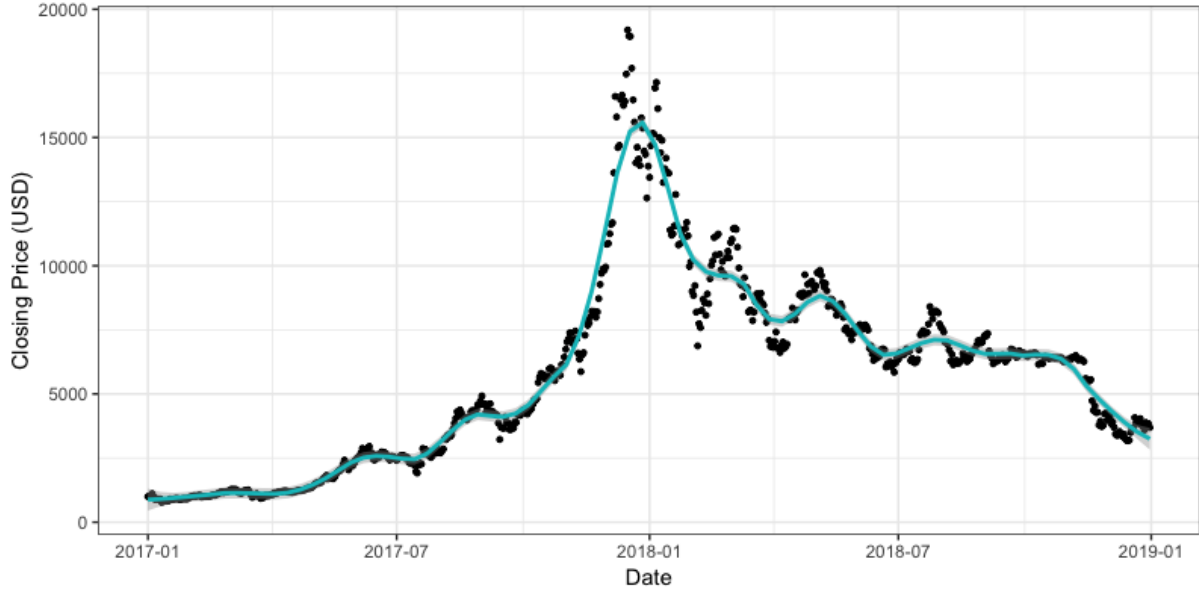


Figure 10: Daily bitcoin closing price with a smoothing line

closing price. Figure 11 illustrates the predicted curves of the LABS and competing models for approximating an unknown function of daily bitcoin closing price. There are no significant differences between the estimated posterior curves.

Alternatively, we calculate cross-validation errors to assess model performances. The values of cross-validation errors are given in Table 6. Both Table 6 and Figure 12 demonstrate that the LABS model provides more accurate function estimation and consistent performance through both minimum mean and relatively low standard deviation values of the cross-validation errors. They also indicate that the Gaussian process is not proper in the cases with locally varying smoothness. We found that the LABS gives more reliable estimated functions that may have both discontinuous and smooth parts than other methods.

	LABS	BASS-1	BPP-21	LARMuK	GP-R
Mean	98014	109222	99937	149272	583046
Standard Deviation	30057	30052.5	29210	51128.7	137859.7

Table 6: Mean and standard deviation for the error rate of 10-folds cross-validation on Bitcoin dataset

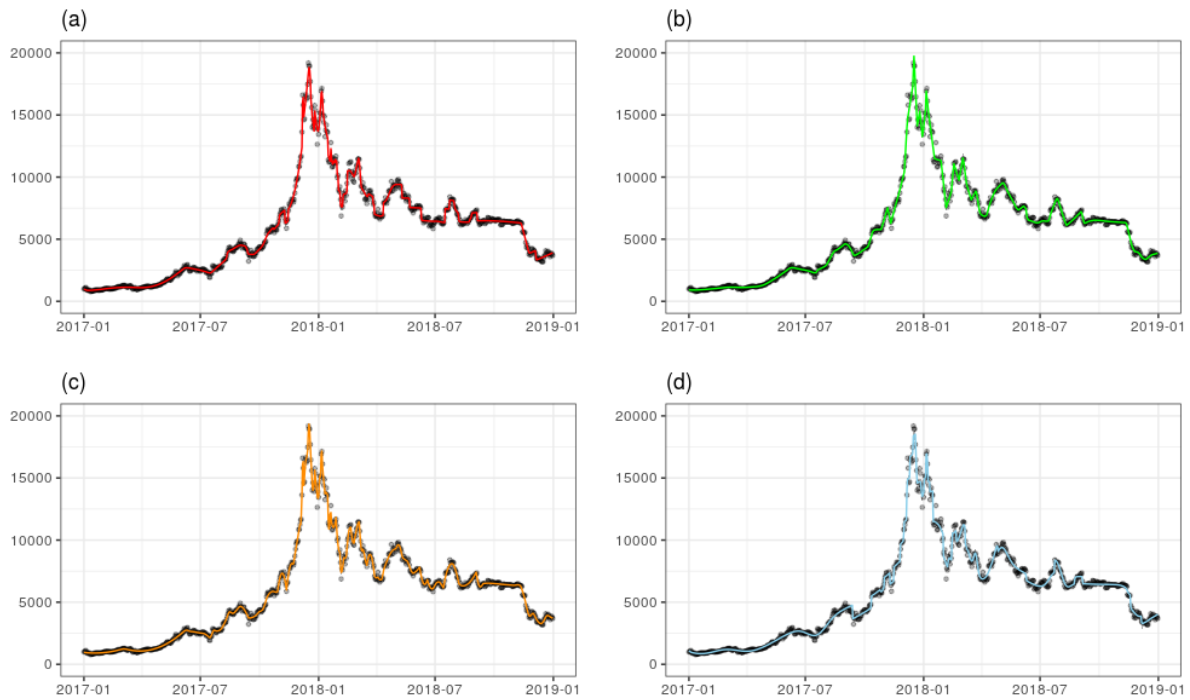


Figure 11: Posterior mean of η on Bitcoin dataset using four models: (a) LABS, (b) BASS-1, (c) BPP-21 and (d) LARMuK

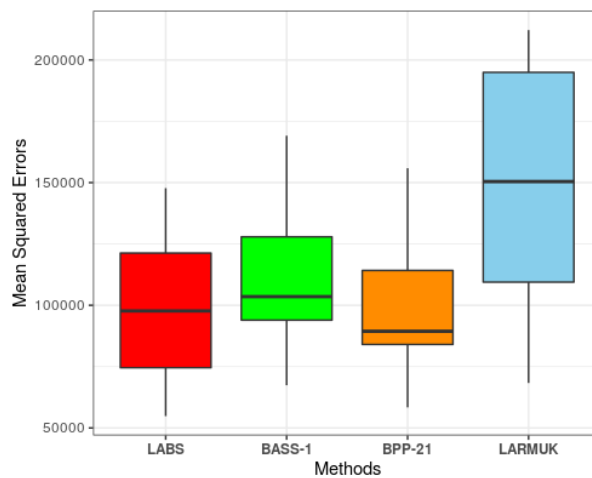


Figure 12: Boxplot of the cross-validation test error rate for the Bitcoin data.

6.3 Example 3: Fine particulate matter in Seoul

The fine dust has become a national issue and its forecast received great attention from the media. A lot of research on fine particulate matter (PM2.5) have been carried out as it gained social attention. According to the studies, Korea's fine dust particles originated from within the country and external sources from China. Many factors cause PM2.5 concentration to rapidly rise or fall and make it difficult to accurately predict the behavior of it.

We estimate the unknown function of daily maximum concentrations of PM2.5 in Seoul. The PM2.5 dataset collected from the AIRKOREA (<https://www.airkorea.or.kr>) includes 1261 daily maximum values of PM2.5 concentration from January 1, 2015, to June 30, 2018. We removed all observations that have missing values.

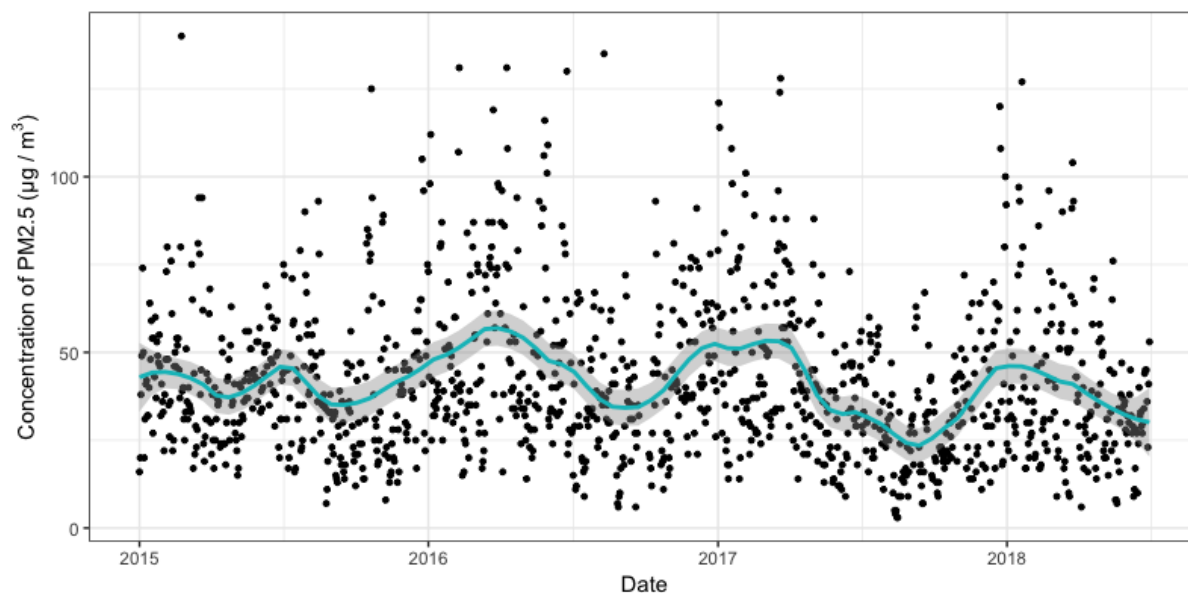


Figure 13: Daily maximum concentrations of PM2.5 in Seoul with a smoothing line

Figure 13 displays daily fluctuations and seasonality. PM2.5 concentrations are higher in winter and spring than in summer and fall. A LOESS smoothed line added in the figure does not reflect these features well. We take advantage of combinations of basis functions, $S = \{0, 1, 2\}$ to grasp such characteristics of PM2.5 data with multiple jumps and peak points. As shown in Figure 14, all four methods represent different estimated lines of the unknown mean function and pick features of the data up in their way. Interestingly, LABS, BASS-1, and BPP-10 react in different ways while they detect peaks, jumps, and smooth parts of PM2.5 data.

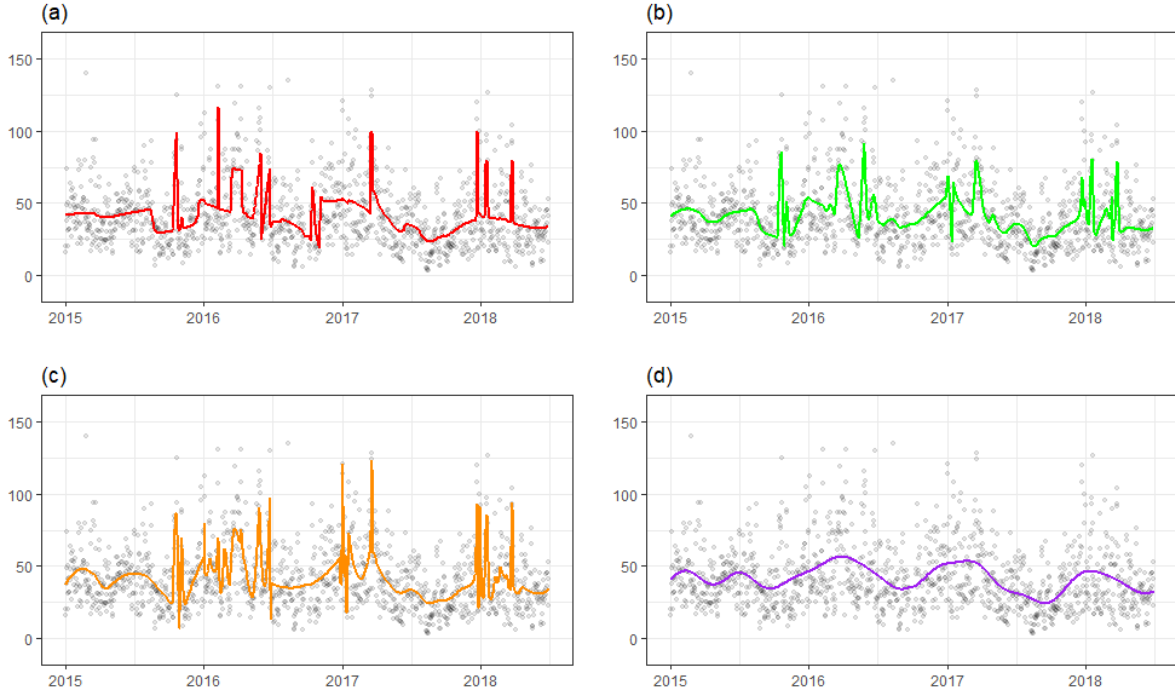


Figure 14: Posterior mean of the mean function on PM2.5 dataset using four models: (a) LABS, (b) BASS-1, (c) BPP-10 and (d) GP-R

We also compute the average and standard deviation of the cross-validated errors of LABS, BPP-10, BASS-1, LARMuK, and GP-R, which are given in Table 7. The LABS model has the lowest cross-validation error among all methods. Moreover a comparably low standard deviation of LABS supports that it has a more stable performance for estimating any shape of functions due to using all three types of B-spline basis.

	LABS	BASS-1	BPP-10	LARMuK	GP-R
Mean	384.8863	393.6049	398.17	399.6718	436.2286
Standard Deviation	56.88069	60.38016	58.63784	53.02499	67.98722

Table 7: Mean and standard deviation for the error rate of 10-folds cross-validation on Seoul PM2.5 dataset

7 Conclusions

We suggested general function estimation methodologies using the B-spline basis function as the elements of an overcomplete system. The B-spline basis can systematically represent functions with varying smoothness since it has nice properties such as local support and differentiability. The overcomplete system and a Lévy random measure enable a function that has both continuous and discontinuous parts to capture all features of the unknown regression function. Simulation studies and real data analysis also present that the proposed models show better performance than other competing models. We also showed that the prior has full support in certain Besov spaces. The prominent limitation of the LABS model is the slow mixing of the MCMC algorithm. Future work will develop an efficient algorithm for the LABS model and extend the LABS model for multivariate analysis.

References

- Abramovich, F., Sapatinas, T. and Silverman, B. W. (1998). Wavelet thresholding via a bayesian approach, *Journal of the Royal Statistical Society: Series B (Statistical Methodology)* **60**(4): 725–749.
- Angrist, J. D. and Pischke, J.-S. (2014). *Mastering'metrics: The path from cause to effect*, Princeton University Press.
- Chu, J.-H., Clyde, M. A. and Liang, F. (2009). Bayesian function estimation using continuous wavelet dictionaries, *Statistica Sinica* pp. 1419–1438.
- Cohen, A. (2003). *Numerical analysis of wavelet methods*, Elsevier.
- Cox, M. G. (1972). The numerical evaluation of b-splines, *IMA Journal of Applied Mathematics* **10**(2): 134–149.
- Crainiceanu, C. M., Ruppert, D., Carroll, R. J., Joshi, A. and Goodner, B. (2007). Spatially adaptive bayesian penalized splines with heteroscedastic errors, *Journal of Computational and Graphical Statistics* **16**(2): 265–288.
- De Boor, C. (1972). On calculating with b-splines, *Journal of Approximation Theory* **6**(1): 50–62.

- Denison, D. G., Mallick, B. K. and Smith, A. F. (1998a). Bayesian mars, *Statistics and Computing* **8**(4): 337–346.
- Denison, D., Mallick, B. and Smith, A. (1998b). Automatic bayesian curve fitting, *Journal of the Royal Statistical Society: Series B (Statistical Methodology)* **60**(2): 333–350.
- DeVore, R. A. and Lorentz, G. G. (1993). *Constructive Approximation*, Vol. 303, Springer Science & Business Media.
- DiMatteo, I., Genovese, C. R. and Kass, R. E. (2001). Bayesian curve-fitting with free-knot splines, *Biometrika* **88**(4): 1055–1071.
- Donoho, D. L. and Johnstone, I. M. (1995). Adapting to unknown smoothness via wavelet shrinkage, *Journal of the american statistical association* **90**(432): 1200–1224.
- Donoho, D. L. and Johnstone, J. M. (1994). Ideal spatial adaptation by wavelet shrinkage, *Biometrika* **81**(3): 425–455.
- Feng, D. (2013). miscf: Miscellaneous functions.
URL: <https://cran.r-project.org/web/packages/miscF>
- Francom, D. and Sanso, B. (2016). Bass: Bayesian adaptive spline surfaces.
URL: <https://cran.r-project.org/web/packages/BASS/>
- Francom, D., Sansó, B., Kupresanin, A. and Johannesson, G. (2018). Sensitivity analysis and emulation for functional data using bayesian adaptive splines, *Statistica Sinica* **28**: 791–816.
- Friedman, J. H. (1991). Multivariate adaptive regression splines, *The annals of statistics* pp. 1–67.
- Gijbels, I., Lambert, A. and Qiu, P. (2007). Jump-preserving regression and smoothing using local linear fitting: a compromise, *Annals of the Institute of Statistical Mathematics* **59**(2): 235–272.
- Green, P. J. (1995). Reversible jump markov chain monte carlo computation and bayesian model determination, *Biometrika* **82**(4): 711–732.

- Johnstone, I. M. and Silverman, B. W. (2005). Empirical bayes selection of wavelet thresholds, *Annals of Statistics* pp. 1700–1752.
- Karatzoglou, A., Smola, A., Hornik, K., Maniscalco, M. A., Teo, C. H. and (NICTA), N. I. A. (2004). kernlab: Kernel-based machine learning lab.
URL: <https://cran.r-project.org/web/packages/kernlab/>
- Koo, J.-Y. (1997). Spline estimation of discontinuous regression functions, *Journal of Computational and Graphical Statistics* **6**(3): 266–284.
- Krivobokova, T., Crainiceanu, C. M. and Kauermann, G. (2008). Fast adaptive penalized splines, *Journal of Computational and Graphical Statistics* **17**(1): 1–20.
- Lee, J. (2007). Sampling methods of neutral to the right processes, *Journal of Computational and Graphical Statistics* **16**(3): 656–671.
- Lee, J. and Kim, Y. (2004). A new algorithm to generate beta processes, *Computational Statistics & Data Analysis* **47**(3): 441–453.
- Lee, T. C. (2002). Automatic smoothing for discontinuous regression functions, *Statistica Sinica* pp. 823–842.
- Lee, Y., Mano, S. and Lee, J. (2020). Bayesian curve fitting for discontinuous functions using an overcomplete system with multiple kernels, *Journal of the Korean Statistical Society* pp. 1–21.
- Lewicki, M. S. and Sejnowski, T. J. (2000). Learning overcomplete representations, *Neural computation* **12**(2): 337–365.
- Liu, Z. and Guo, W. (2010). Data driven adaptive spline smoothing, *Statistica Sinica* pp. 1143–1163.
- Luo, Z. and Wahba, G. (1997). Hybrid adaptive splines, *Journal of the American Statistical Association* **92**(437): 107–116.
- Ouyang, Z., Clyde, M. A. and Wolpert, R. L. (2008). *Bayesian additive regression kernels*, Duke University.

- Petrushev, P. P. (1988). Direct and converse theorems for spline and rational approximation and besov spaces, *Function spaces and applications*, Springer, pp. 363–377.
- Pillai, N. S. (2008). *Lévy random measures: Posterior consistency and applications*, PhD dissertation, Duke University.
- Pillai, N. S., Wu, Q., Liang, F., Mukherjee, S. and Wolpert, R. L. (2007). Characterizing the function space for bayesian kernel models, *Journal of Machine Learning Research* **8**(Aug): 1769–1797.
- Pintore, A., Speckman, P. and Holmes, C. C. (2006). Spatially adaptive smoothing splines, *Biometrika* **93**(1): 113–125.
- Qiu, P. (2003). A jump-preserving curve fitting procedure based on local piecewise-linear kernel estimation, *Journal of Nonparametric Statistics* **15**(4-5): 437–453.
- Qiu, P. and Yandell, B. (1998). Local polynomial jump-detection algorithm in nonparametric regression, *Technometrics* **40**(2): 141–152.
- R Core Team (2020). *R: A Language and Environment for Statistical Computing*, R Foundation for Statistical Computing, Vienna, Austria.
URL: <http://www.R-project.org/>
- Ruppert, D. and Carroll, R. J. (2000). Theory & methods: Spatially-adaptive penalties for spline fitting, *Australian & New Zealand Journal of Statistics* **42**(2): 205–223.
- Silverman, B. W., Evers, L., Xu, K., Carbonetto, P. and Stephens, M. (2005). Ebayesthresh: Empirical bayes thresholding and related methods.
URL: <https://cran.r-project.org/web/packages/EbayesThresh/>
- Simoncelli, E. P., Freeman, W. T., Adelson, E. H. and Heeger, D. J. (1992). Shiftable multiscale transforms, *IEEE Transactions on Information Theory* **38**(2): 587–607.
- Smith, M. and Kohn, R. (1996). Nonparametric regression using bayesian variable selection, *Journal of Econometrics* **75**(2): 317–343.

- Tu, C. (2006). *Bayesian nonparametric modeling using Levy process priors with applications for function estimation, time series modeling and spatio-temporal modeling*, PhD dissertation, Duke University.
- Wang, X., Du, P. and Shen, J. (2013). Smoothing splines with varying smoothing parameter, *Biometrika* **100**(4): 955–970.
- Wang, X.-F. (2010). fancova: Nonparametric analysis of covariance.
URL: <https://cran.r-project.org/web/packages/fANCOVA/>
- Wolpert, R. L., Clyde, M. A., Tu, C. et al. (2011). Stochastic expansions using continuous dictionaries: Lévy adaptive regression kernels, *The Annals of Statistics* **39**(4): 1916–1962.
- Xia, Z. and Qiu, P. (2015). Jump information criterion for statistical inference in estimating discontinuous curves, *Biometrika* **102**(2): 397–408.
- Yang, L. and Hong, Y. (2017). Adaptive penalized splines for data smoothing, *Computational Statistics & Data Analysis* **108**: 70–83.
- Yang, Y. and Song, Q. (2014). Jump detection in time series nonparametric regression models: a polynomial spline approach, *Annals of the Institute of Statistical Mathematics* **66**(2): 325–344.
- Zhou, S. and Shen, X. (2001). Spatially adaptive regression splines and accurate knot selection schemes, *Journal of the American Statistical Association* **96**(453): 247–259.

A Proof of Theorems 1-3

A.1 Proof of Theorem 1

For simplicity, we assume that $\mathcal{X} = [0, 1]$. Since the B-spline basis has local support and is bounded, $\|B_k(x; \boldsymbol{\xi}_k)\|_p$ is finite for all $k \geq 0$. It is enough to show that if the Besov semi-norm, $|B_k(x; \boldsymbol{\xi}_k)|_{\mathbb{B}_{p,q}^\alpha}$ is finite for all $k \geq 0$. The definition of the modulus of smoothness and the property that $\omega_k(f, t)_p \leq 2^r \cdot \omega_{k-r}(f, t)_p$, $0 \leq r \leq k$, if $f \in L_p(\mathcal{X})$ imply that

$$\omega_r(B_k(x; \boldsymbol{\xi}_k), t)_p \leq 2^{r-1} \cdot \omega_1(B_k(x; \boldsymbol{\xi}_k), t)_p.$$

Let k be zero. Then, the B-spline basis is piecewise constant with 2 knots, $\boldsymbol{\xi}_0 := (\boldsymbol{\xi}_{01}, \boldsymbol{\xi}_{02})$. By the definition of the B-spline basis (6), we divide into two cases to calculate the modulus of continuity.

Case 1 Assume $\boldsymbol{\xi}_{01} + h < \boldsymbol{\xi}_{02}$, $h > 0$. Thus,

$$\|B_0(x + h; \boldsymbol{\xi}_0) - B_0(x; \boldsymbol{\xi}_0)\|_p \leq 2 \cdot h^{\frac{1}{p}}.$$

Case 2 Assume $\boldsymbol{\xi}_{01} + h > \boldsymbol{\xi}_{02}$, $h > 0$. Thus,

$$\|B_0(x + h; \boldsymbol{\xi}_0) - B_0(x; \boldsymbol{\xi}_0)\|_p \leq 2 \cdot h^{\frac{1}{p}}.$$

Therefore, in all cases,

$$\omega_r(B_0(x; \boldsymbol{\xi}_0), t)_p \leq 2^r \cdot h^{\frac{1}{p}}. \quad (17)$$

By definition, $|B_0(x; \boldsymbol{\xi}_0)|_{\mathbb{B}_{p,q}^\alpha} = \left(\int_0^\infty (t^{-s} \omega_r(B_0(x; \boldsymbol{\xi}_0), t)_p)^p \frac{dt}{t} \right)^{1/q}$, so

$$\begin{aligned} |B_0(x; \boldsymbol{\xi}_0)|_{\mathbb{B}_{p,q}^\alpha} &\leq \left[\int_0^1 t^{-sq-1} \cdot 2^{rq} \cdot t^{\frac{1}{p}} dt + \int_1^\infty t^{-sq-1} \cdot 2^{rq} dt \right]^{1/q} \\ &= 2^r \cdot \left[\int_0^1 t^{-q(s-\frac{1}{p})-1} dt + \int_1^\infty t^{-sq-1} dt \right]^{1/q}. \end{aligned}$$

The upper bound of $|B_0(x; \boldsymbol{\xi}_0)|_{\mathbb{B}_{p,q}^\alpha}$ is finite if and only if $\alpha < \frac{1}{p}$ and $q < \infty$.

Let $k \geq 1$. Since the B-spline basis of order k is a piecewise polynomial and has $(k - 1)$ continuous derivatives at the knots, it falls in $W_p^k(\mathcal{X})$, where $W_p^k(\mathcal{X})$ is the Sobolev space, which is a vector space of functions that have weak derivatives. See the definition of the Sobolev space

described in chapter 2.5 of DeVore and Lorentz (1993). We use the following property of the modulus of smoothness,

$$\omega_{r+k}(f, t)_p \leq t^r \cdot \omega_k(f^{(r)}, t)_p, t > 0,$$

where $f^{(r)}$ is the weak r th derivative of f . For $k \geq 1$, the Besov semi-norm of $B_k(x; \boldsymbol{\xi}_k)$ is bounded by

$$\begin{aligned} |B_k(x; \boldsymbol{\xi}_k)|_{\mathbb{B}_{p,q}^\alpha} &= \left(\int_0^\infty (t^{-\alpha} \omega_r(B_k(x; \boldsymbol{\xi}_k), t)_p)^q \frac{dt}{t} \right)^{1/q} \\ &\leq \left(\int_0^1 (t^{-\alpha} \cdot (t^k \cdot \omega_{r-k}(B_k^{(k)}(x; \boldsymbol{\xi}_k), t)_p)^q \frac{dt}{t} + \int_1^\infty 2^{rq} \cdot t^{-sq-1} dt \right)^{1/q} \\ &\leq \left(\int_0^1 (t^{-\alpha q-1} \cdot (t^k \cdot 2^{r-k-1} \cdot \omega_1(B_k^{(k)}(x; \boldsymbol{\xi}_k), t)_p)^q dt + 2^{rq} \cdot \int_1^\infty t^{-\alpha q-1} dt \right)^{1/q} \end{aligned} \quad (18)$$

Since $B_k^{(k)}(x; \boldsymbol{\xi}_k)$ is a piecewise constant function, (17) implies that

$$\omega_1(B_k^{(k)}(x; \boldsymbol{\xi}_k), t)_p \leq C \cdot h^{\frac{1}{p}}, \quad \text{for some constant } C > 0. \quad (19)$$

Using (18) and (19), it follows that

$$|B_k(x; \boldsymbol{\xi}_k)|_{\mathbb{B}_{p,q}^\alpha} \leq \left(C' \cdot \int_0^1 t^{-\alpha q + kq + \frac{q}{p} - 1} dt + 2^{rq} \cdot \int_1^\infty t^{-\alpha q - 1} dt \right)^{1/q}, \quad \text{for some constant } C' > 0.$$

For all $k \geq 1$, $|B_k(x; \boldsymbol{\xi}_k)|_{\mathbb{B}_{p,q}^\alpha}$ is finite if and only if $\alpha < k + \frac{1}{p}$ and $q < \infty$, so the proof is complete.

A.2 Proof of Theorem 2

By Theorem 3 of Wolpert et al. (2011), the L_p norm and Besov semi-norm of η satisfy the following upper bounds, respectively.

$$\begin{aligned} \|\eta\|_p &\leq \sum_{k \in S} \sum_l \|B_k(x; \boldsymbol{\xi}_{k,l})\|_p |\beta_{k,l}|, \\ |\eta|_{\mathbb{B}_{p,q}^\alpha} &\leq \sum_{k \in S} \sum_l |\beta_{k,l}| \cdot |B_k|_{\mathbb{B}_{p,q}^\alpha}, \end{aligned}$$

Since the condition for (12) is satisfied and B-spline basis is bounded and locally supported, $\|\eta\|_p$ is almost surely finite. To obtain finite Besov semi-norms for all $k \in S$, the smoothness parameter α should be $\alpha < \min(S) + \frac{1}{p}$ by Theorem 1. Therefore, η belongs to $\mathbb{B}_{p,q}^\alpha$ with $\alpha < \min(S) + \frac{1}{p}$ almost surely.

A.3 Proof of Theorem 3

For the sake of simplicity we assume $\mathcal{X} = [0, 1]$. Fix $\delta > 0$ and $\eta_0 \in \mathbb{B}_{p,q}^\alpha([0, 1])$ with $\alpha > 0, 1 \leq p, q < \infty$. If $1 \leq p' \leq p < \infty$, then η_0 also belongs to $\mathbb{B}_{p',q}^\alpha([0, 1])$ by property of the Besov space (Cohen; 2003)[3.2, page 163]. From Theorem 2.1 of Petrushev (1988), we can show that there exists a spline $s \in S(n^*, q)$ such that

$$\|\eta_0 - s\|_p < C \frac{\|\eta_0\|_{\mathbb{B}_{p',q}^\alpha}}{(n^*)^\alpha} < \frac{\delta}{2},$$

where $S(n^*, q)$ denotes the set of all splines of degree $(q - 1)$ with a sufficiently large number n^* knots and constant $C = C(\alpha, p, q)$. Since any spline of given degree can be represented as a linear combination of B-spline basis functions with same degree, we can define a spline $s(x)$ by

$$s(x) = \sum_{j=1}^{n^*} \beta_j^* B_{(q-1),j}^*(x), \quad (20)$$

where $B_{(q-1),j}^*(x)$ is the B-spline basis of degree $(q - 1)$ with a sequence of knots $\boldsymbol{\xi}^*$ in (6).

Set $n^* := \sum_{k \in S} J_k^\delta$, $A := \sum_{k \in S} \sum_{l=1}^{J_k^\delta} |\beta_{k,l}| < \infty$, $\rho := \sup \|B_k(x, \boldsymbol{\xi}_k)\|_p < \infty$ and $\epsilon := \frac{\delta}{2(A+\rho)}$. We denote the range of a sequence of knots $\boldsymbol{\xi}_{k,l}$ by $r(\boldsymbol{\xi}_{k,l})$, e.g., $r(\boldsymbol{\xi}_{k,l}) = (\xi_{k,l,(k+2)} - \xi_{k,l,1})$. For convenience, we reindex the coefficients and knots of the spline $s(x)$ in (20) such that $\beta_{k,l}^*$ and $\boldsymbol{\xi}_{k,l}^*$ for $l = 1, \dots, J_k^\delta, k \in S$. Then, the spline $s(x)$ can be expressed as follows:

$$s(x) = \sum_{k \in S} \sum_{l=1}^{J_k^\delta} \beta_{k,l}^* B_{(q-1),l}^*(x; \boldsymbol{\xi}_{k,l}^*),$$

where $\boldsymbol{\xi}_{k,l}^* := (\xi_l^*, \dots, \xi_{l+(q-1)+1}^*)$ is a subsequence of given knots $\boldsymbol{\xi}^*$. Using the definitions of B-spline basis in (6) and (7), we can find a $\zeta > 0$ such that

$$\max(r(\boldsymbol{\xi}_{k,l}), r(\boldsymbol{\xi}_{k,l}^*)) < \zeta \Rightarrow \|B_k(x; \boldsymbol{\xi}_{k,l}) - B_{(q-1),l}^*(x; \boldsymbol{\xi}_{k,l}^*)\|_p < \epsilon, \quad \forall l, \forall k.$$

Let's define the set

$$\bar{b}'(\eta_0) := \left\{ \eta : \eta(x) = \sum_{k \in S} \sum_{l=1}^{J_k^\delta} \beta_{k,l} B_k(x; \boldsymbol{\xi}_{k,l}), \sum_{k \in S} \sum_{l=1}^{J_k^\delta} |\beta_{k,l} - \beta_{k,l}^*| < \epsilon, \max(r(\boldsymbol{\xi}_{k,l}), r(\boldsymbol{\xi}_{k,l}^*)) < \zeta, \forall l, \forall k \right\}.$$

Lemma 4

$$\bar{b}'_\delta(\eta_0) \subset \bar{b}_\delta(\eta_0)$$

Proof It suffices to show that $\eta \in \bar{b}'_\delta(\eta_0) \implies \eta \in \bar{b}_\delta(\eta_0)$ to finish the proof of the lemma. For any $\eta \in \bar{b}'_\delta(\eta_0)$,

$$\begin{aligned} \|\eta - s\|_p &\leq \sum_{k \in S} \sum_{l=1}^{J_k^\delta} \|\beta_{k,l} B_k(x; \boldsymbol{\xi}_{k,l}) - \beta_{k,l}^* B_{(q-1),l}^*(x; \boldsymbol{\xi}_{k,l}^*)\|_p \\ &\leq \sum_{k \in S} \sum_{l=1}^{J_k^\delta} |\beta_{k,l}| \cdot \|B_k(x; \boldsymbol{\xi}_{k,l}) - B_{(q-1),l}^*(x; \boldsymbol{\xi}_{k,l}^*)\|_p + \sum_{k \in S} \sum_{l=1}^{J_k^\delta} |\beta_{k,l} - \beta_{k,l}^*| \cdot \|B_k(x; \boldsymbol{\xi}_{k,l})\|_p \\ &\leq \epsilon \cdot \sum_{k \in S} \sum_{l=1}^{J_k^\delta} |\beta_{k,l}| + \rho \cdot \sum_{k \in S} \sum_{l=1}^{J_k^\delta} |\beta_{k,l} - \beta_{k,l}^*| \\ &\leq \epsilon \cdot A + 2\rho \cdot \epsilon = (A + \rho) \cdot \epsilon = \frac{\delta}{2}. \end{aligned}$$

By the triangle inequality,

$$\begin{aligned} \|\eta - \eta_0\|_p &\leq \|\eta - s\|_p + \|s - \eta_0\|_p \\ &< \frac{\delta}{2} + \frac{\delta}{2} = \delta. \end{aligned}$$

Thus, $\eta \in \bar{b}_\delta(\eta_0)$ and this finishes the proof of the lemma.

To complete the proof of this theorem, we have to show that $\Pi(\eta \in \bar{b}'_\delta(\eta_0)) > 0$ by using the previous lemma. Let $J^* := \max_{k \in S} J_k^\delta$. By the triangle inequality,

$$\begin{aligned}
\Pi(\eta \in \bar{b}'_\delta(\eta_0)) &= \Pi\left(\sum_{k \in S} \int \int_{\mathbf{R} \times \mathcal{X}^{(k+2)}} \beta_k B_k(x; \boldsymbol{\xi}_k) N_k(d\beta_k, d\boldsymbol{\xi}_k) \in \bar{b}'_\delta(\eta_0)\right) \\
&= \Pi\left(\sum_{k \in S} \sum_{l=1}^{J_k} B_k(x; \boldsymbol{\xi}_{k,l}) \beta_{k,l} \in \bar{b}'_\delta(\eta_0)\right) \\
&= \mathbb{P}\left[\sum_{k \in S} \sum_{l=1}^{J_k^\delta} |\beta_{k,l} - \beta_{k,l}^*| < \epsilon, \max(r(\boldsymbol{\xi}_{k,l}), r(\boldsymbol{\xi}_{k,l}^*)) < \zeta, J_k = J_k^\delta, \forall k \in S\right] \\
&> \prod_{k \in S} \left\{ \mathbb{P}\left[|\beta_{k,l} - \beta_{k,l}^*| < \frac{\epsilon}{|S|J^*}, \max(r(\boldsymbol{\xi}_{k,l}), r(\boldsymbol{\xi}_{k,l}^*)) < \zeta, l = 1, 2, \dots, J_k^\delta\right] \right\} \\
&\quad \times \prod_{k \in S} \left[\frac{\nu_k(\mathbb{R} \times \mathcal{X}^{(k+2)})^{J_k^\delta} \cdot \exp(-\nu_k(\mathbb{R} \times \mathcal{X}^{(k+2)}))}{J_k^{\delta!}} \right] \\
&= \prod_{k \in S} \left\{ \prod_{j=1}^{J_k^\delta} \left[\frac{\nu_k(|\beta_{k,l} - \beta_{k,l}^*| < \frac{\epsilon}{|S|J^*}, \max(r(\boldsymbol{\xi}_{k,l}), r(\boldsymbol{\xi}_{k,l}^*)) < \zeta)}{\nu_k(\mathbb{R} \times \mathcal{X}^{(k+2)})} \right] \right\} \\
&\quad \times \prod_{k \in S} \left[\frac{\nu_k(\mathbb{R} \times \mathcal{X}^{(k+2)})^{J_k^\delta} \cdot \exp(-\nu_k(\mathbb{R} \times \mathcal{X}^{(k+2)}))}{J_k^{\delta!}} \right] \\
&= \prod_{k \in S} \left\{ \prod_{j=1}^{J_k^\delta} \left[\int_{|\beta_{k,l} - \beta_{k,l}^*| < \frac{\epsilon}{|S|J^*}} \pi(\beta_k) d\beta_k \int_{\max(r(\boldsymbol{\xi}_{k,l}), r(\boldsymbol{\xi}_{k,l}^*)) < \zeta} \pi(\boldsymbol{\xi}_k) d\boldsymbol{\xi}_k \right] \times \left[\frac{M_k^{J_k^\delta} \cdot \exp(-M_k)}{J_k^{\delta!}} \right] \right\}.
\end{aligned}$$

Since we assume a finite Levy measure and $\pi(\beta_k) = \mathcal{N}(\beta_k; 0, \phi_k^2)$, $\pi(\boldsymbol{\xi}_k) = \mathcal{U}(\mathcal{X}^{(k+2)})$ in the LABS model,

$$\Pi(\eta \in \bar{b}'_\delta(\eta_0)) > 0.$$

Hence, by applying the lemma, we get $\Pi(\eta \in \bar{b}_\delta(\eta_0)) \geq \Pi(\eta \in \bar{b}'_\delta(\eta_0)) > 0$ and the theorem is proved.

B Full simulation results for Simulation 1

This appendix contains the full simulations results of the four DJ test functions. We simulated two scenarios: (a) small sample size ($n = 128$) and (b) large sample size ($n = 512$) with different noise levels (RSNR = 3, 5, and 10).

Model	Bumps			Blocks		
	RSNR=3	RSNR=5	RSNR=10	RSNR=3	RSNR=5	RSNR=10
BSP-2	26.904(0.4461)	25.495(0.1606)	24.9(0.0401)	5.96(0.4429)	4.53(0.1594)	3.927(0.0399)
LOESS	47.266(0.1618)	47.163(0.0812)	47.119(0.0366)	17.924(0.7218)	17.503(0.3846)	17.332(0.2312)
SS	43.552(4.6764)	43.377(4.7159)	43.984(4.6074)	4.895(0.5145)	3.396(0.241)	2.699(0.1107)
NWK	39.892(1.8831)	39.365(1.3862)	39.033(0.7393)	4.285(0.7336)	1.936(0.36)	0.472(0.0567)
EBW	4.986(1.1761)	1.936(0.601)	0.447(0.0981)	3.243(1.0747)	0.859(0.2237)	0.21(0.0484)
GSP-L	22.99(4.8847)	22.03(5.3556)	20.112(4.4213)	7.409(1.3261)	6.637(0.9807)	6.546(1.1115)
GSP-R	41.626(2.9041)	40.819(2.7234)	40.955(3.102)	15.654(2.0255)	15.323(1.8902)	15.44(2.3391)
BPP-10	4.571(2.3604)	3.668(2.7142)	3.304(2.9789)	2.156(0.789)	0.908(0.2537)	0.465(0.2403)
BPP-21	15.115(5.9376)	14.674(6.3396)	14.363(6.7395)	3.918(0.589)	2.682(0.5399)	2.311(0.451)
BASS-1	2.968(0.4322)	1.206(0.4907)	0.252(0.0421)	2.498(0.6331)	0.696(0.2226)	0.122(0.0381)
BASS-2	47.977(7.4411)	45.988(9.3435)	45.021(9.2185)	7.533(1.7616)	4.253(0.8586)	2.852(0.3863)
LARMuK	2.852(0.426)	1.182(0.678)	0.319(0.0663)	1.799(0.5873)	0.682(0.2436)	0.193(0.08)
LABS	2.589(0.5908)	0.837(0.3124)	0.246(0.0683)	1.305(0.5272)	0.365(0.1645)	0.072(0.0293)

Table 8: Average mean squared errors with estimated standard errors in parentheses from 100 replications for Bumps and Blocks examples with $n = 128$

Model	Doppler			Heavisine		
	RSNR=3	RSNR=5	RSNR=10	RSNR=3	RSNR=5	RSNR=10
BSP-2	3.896(0.4928)	2.447(0.1774)	1.836(0.0444)	2.399(0.4208)	0.926(0.1515)	0.305(0.0379)
LOESS	8.891(1.506)	6.533(1.0853)	5.344(0.6362)	0.895(0.2248)	0.548(0.0976)	0.35(0.0436)
SS	3.644(0.587)	2.025(0.24)	1.251(0.0812)	0.875(0.2725)	0.484(0.1021)	0.235(0.0299)
NWK	4.045(1.102)	1.864(0.2683)	0.477(0.0624)	1.022(0.352)	0.521(0.1321)	0.228(0.0472)
EBW	2.979(0.6397)	1.319(0.3142)	0.341(0.0855)	1.29(0.3473)	0.586(0.1365)	0.185(0.0456)
GSP-L	5.845(1.3505)	5.313(1.3217)	4.843(0.9023)	2.601(2.0255)	2.217(2.1273)	1.743(1.7561)
GSP-R	12.164(2.9995)	11.588(3.1093)	12.402(3.5243)	1.02(0.2869)	0.756(0.1707)	0.646(0.1152)
BPP-10	2.911(0.6396)	1.275(0.2471)	0.559(0.2008)	1.503(0.4239)	0.674(0.1576)	0.217(0.0616)
BPP-21	2.575(0.5217)	1.463(0.3399)	1.166(0.3932)	0.941(0.2702)	0.444(0.105)	0.147(0.032)
BASS-1	2.865(0.6162)	1.167(0.2607)	0.353(0.0605)	1.022(0.2434)	0.499(0.1047)	0.135(0.033)
BASS-2	2.841(0.5796)	1.753(0.2702)	1.344(0.1205)	0.802(0.2053)	0.452(0.0953)	0.176(0.0399)
LARMuK	3(0.6708)	1.212(0.3684)	0.364(0.1179)	1.13(0.3235)	0.541(0.16)	0.164(0.0566)
LABS	2.273(0.568)	0.848(0.2521)	0.234(0.0551)	0.897(0.242)	0.413(0.1492)	0.103(0.0406)

Table 9: Average mean squared errors with estimated standard errors in parentheses from 100 replications for Doppler and Heavisine examples with $n = 128$

Model	Bumps			Blocks		
	RSNR=3	RSNR=5	RSNR=10	RSNR=3	RSNR=5	RSNR=10
BSP-2	29.359(0.1163)	29.011(0.0419)	28.864(0.0105)	5.097(0.118)	4.74(0.0425)	4.59(0.0106)
LOESS	43.468(5.4554)	40.385(7.3012)	36.495(7.2734)	3.755(0.2529)	3.095(0.1343)	2.922(0.0252)
SS	16.211(0.255)	15.406(0.123)	15.06(0.0537)	2.837(0.1609)	2.197(0.0713)	1.883(0.0256)
NWK	4.885(0.3559)	1.796(0.1194)	0.482(0.0319)	2.34(0.1831)	1.349(0.1149)	0.581(0.1147)
EBW	2.42(0.3291)	0.914(0.0992)	0.272(0.0279)	1.227(0.2009)	0.398(0.0753)	0.088(0.0177)
GSP-L	16.704(2.5691)	16.212(2.324)	16.224(2.5594)	3.089(0.342)	2.613(0.3006)	2.522(0.3358)
GSP-R	39.297(1.3464)	39.046(1.3386)	38.885(1.2831)	13.847(1.3079)	13.783(1.3156)	13.622(1.2962)
BPP-10	1.9(0.6277)	1.429(0.6619)	1.352(0.8161)	0.493(0.137)	0.216(0.0819)	0.182(0.0848)
BPP-21	4.698(0.9928)	4.428(1.1195)	4.308(1.1065)	1.385(0.1974)	0.845(0.127)	0.665(0.1055)
BASS-1	2.497(0.5322)	1.679(0.4936)	1.356(0.559)	0.942(0.195)	0.436(0.1189)	0.273(0.1078)
BASS-2	24.925(2.6356)	23.806(2.8435)	23.387(2.6943)	3.033(0.2242)	2.613(0.182)	2.426(0.1763)
LARMuK	3.692(1.7663)	2.465(1.0197)	1.999(0.7813)	1.074(0.392)	0.646(0.2521)	0.395(0.1903)
LABS	1.371(0.6845)	0.619(0.1769)	0.341(0.1905)	0.363(0.1391)	0.113(0.0562)	0.021(0.009)

Table 10: Average mean squared errors with estimated standard errors in parentheses from 100 replications for Bumps and Blocks examples with $n = 512$

Model	Doppler			Heavisine		
	RSNR=3	RSNR=5	RSNR=10	RSNR=3	RSNR=5	RSNR=10
BSP-2	2.875(0.1038)	2.534(0.0374)	2.39(0.0093)	0.635(0.1112)	0.294(0.04)	0.15(0.01)
LOESS	2.756(0.3006)	2.044(0.0474)	1.893(0.0202)	0.464(0.067)	0.306(0.0523)	0.172(0.0531)
SS	1.993(0.1234)	1.385(0.0531)	1.086(0.0174)	0.384(0.0699)	0.225(0.0299)	0.113(0.0102)
NWK	1.649(0.1233)	0.853(0.105)	0.431(0.0289)	0.398(0.0789)	0.223(0.0327)	0.106(0.0113)
EBW	1.263(0.1618)	0.592(0.0809)	0.156(0.0209)	0.435(0.1007)	0.202(0.0457)	0.066(0.0127)
GSP-L	2.167(0.2292)	1.767(0.2376)	1.621(0.2526)	0.785(0.246)	0.402(0.1555)	0.261(0.1383)
GSP-R	9.389(1.6093)	9.432(1.6343)	9.1(1.577)	0.422(0.0677)	0.322(0.0409)	0.279(0.0372)
BPP-10	1.36(0.1866)	0.632(0.0819)	0.22(0.0283)	0.431(0.1015)	0.173(0.0392)	0.055(0.0108)
BPP-21	1.055(0.1663)	0.496(0.0768)	0.249(0.0468)	0.308(0.0771)	0.134(0.0328)	0.04(0.0091)
BASS-1	1.116(0.1587)	0.602(0.064)	0.363(0.024)	0.365(0.0894)	0.149(0.0348)	0.046(0.011)
BASS-2	1.051(0.1916)	0.588(0.0804)	0.451(0.0613)	0.354(0.0709)	0.169(0.0385)	0.063(0.0131)
LARMuK	1.584(0.2401)	1.04(0.1675)	0.652(0.1067)	0.413(0.1155)	0.19(0.0543)	0.074(0.0206)
LABS	1.243(0.2135)	0.66(0.1141)	0.343(0.0843)	0.291(0.1185)	0.103(0.0508)	0.031(0.0128)

Table 11: Average mean squared errors with estimated standard errors in parentheses from 100 replications for Doppler and Heavisine examples with $n = 512$

C Derivation of the full conditionals for LABS

In this appendix, we derive the full conditional distributions of some parameters required for Gibbs sampling. The full conditional posterior of each parameter can be easily obtained via conjugacy properties. Let us first find the full conditional posterior for $\beta_{p,q}$.

- Full conditional posterior for $\beta_{p,q}$

For each $q = 1, \dots, J_p$,

$$\begin{aligned} [\beta_{p,q} | \beta_{p,-q}, \text{others}, \mathbf{Y}] &\propto \left[\exp \left\{ -\frac{1}{2\sigma^2} \sum_{i=1}^n (y_i - \beta_0 - \sum_{k \in S} \sum_{l=1}^{J_k} B_{k,l}(x_i; \boldsymbol{\xi}_{k,l}) \beta_{k,l})^2 \right\} \right] \times \left[\exp \left\{ -\sum_{k \in S} \sum_{l=1}^{J_k} \frac{\beta_{k,l}^2}{2\sigma_k^2} \right\} \right] \\ &\propto \exp \left\{ -\frac{1}{2\sigma^2} \sum_{i=1}^n (y_i - \beta_0 - \sum_{k \in S \setminus \{p\}} \sum_{l=1}^{J_k} B_{k,l}(x_i; \boldsymbol{\xi}_{k,l}) \beta_{k,l} - \sum_{l=1}^{J_p} B_{p,l}(x_i; \boldsymbol{\xi}_{p,l}) \beta_{p,l})^2 - \frac{1}{2\sigma_p^2} \sum_{k=1}^{J_p} \beta_{p,l}^2 \right\} \end{aligned}$$

For convenience, we set $c_i = \beta_0 + \sum_{k \in S \setminus \{p\}} \sum_{l=1}^{J_k} B_{k,l}(x_i; \boldsymbol{\xi}_{k,l}) \beta_{k,l}$ as a constant term.

Then,

$$\begin{aligned} &\propto \exp \left\{ -\frac{1}{2\sigma^2} \sum_{i=1}^n (y_i - c_i - \sum_{l=1}^{J_p} B_{p,l}(x_i; \boldsymbol{\xi}_{p,l}) \beta_{p,l})^2 - \frac{1}{2\sigma_p^2} \sum_{l=1}^{J_p} \beta_{p,l}^2 \right\} \\ &\propto \exp \left\{ -\frac{1}{2\sigma^2} \sum_{i=1}^n (y_i - c_i - \sum_{l \neq q}^{J_p} B_{p,l}(x_i; \boldsymbol{\xi}_{p,l}) \beta_{p,l} - B_{p,q}(x_i; \boldsymbol{\xi}_{p,q}) \beta_{p,q})^2 - \frac{\beta_{p,q}^2}{2\sigma_p^2} \right\} \\ &\propto \exp \left\{ -\frac{1}{2\sigma^2} \left(\beta_{p,q}^2 \sum_{i=1}^n (B_{p,q}(x_i; \boldsymbol{\xi}_{p,q}))^2 - 2\beta_{p,q} \sum_{i=1}^n \left(y_i - c_i - \sum_{l \neq q}^{J_p} B_{p,l}(x_i; \boldsymbol{\xi}_{p,l}) \beta_{p,l} \right) \times B_{p,q}(x_i; \boldsymbol{\xi}_{p,q}) \right) - \frac{\beta_{p,q}^2}{2\sigma_p^2} \right\} \\ &= \exp \left\{ -\frac{1}{2} \left(\left(\frac{\sum_{i=1}^n (B_{p,q}(x_i; \boldsymbol{\xi}_{p,q}))^2}{\sigma^2} + \frac{1}{\sigma_p^2} \right) \beta_{p,q}^2 - 2 \frac{\sum_{i=1}^n (y_i - c_i - \sum_{l \neq q}^{J_p} B_{p,l}(x_i; \boldsymbol{\xi}_{p,l}) \beta_{p,l}) (B_{p,q}(x_i; \boldsymbol{\xi}_{p,q}))}{\sigma^2} \beta_{p,q} \right) \right\} \end{aligned}$$

Thus, the full conditional distribution for $\beta_{p,q}$ is

$$[\beta_{p,q} | \beta_{p,-q}, \text{others}, \mathbf{Y}] \sim \mathcal{N}(\mu_{p_0}, \sigma_{p_0}^2)$$

with

$$\begin{aligned} \sigma_{p_0}^2 &= \left(\frac{\sum_{i=1}^n (B_{p,q}(x_i; \boldsymbol{\xi}_{p,q}))^2}{\sigma^2} + \frac{1}{\sigma_p^2} \right)^{-1} \\ \mu_{p_0} &= \sigma_{p_0}^2 \times \frac{\sum_{i=1}^n (y_i - c_i - \sum_{l \neq q}^{J_p} B_{p,l}(x_i; \boldsymbol{\xi}_{p,l}) \beta_{p,l}) (B_{p,q}(x_i; \boldsymbol{\xi}_{p,q}))}{\sigma^2}. \end{aligned}$$

- Full conditional posterior of M_k

For each $k \in S$,

$$\begin{aligned} [M_k \mid \text{others}] &\propto M_k^{J_k} \exp\{-M_k\} \times M_k^{a_{\gamma_k}-1} \exp\{-b_{\gamma_k} M_k\} \\ &= M_k^{J_k+a_{\gamma_k}-1} \exp\{-(1+b_{\gamma_k})M_k\} \end{aligned}$$

The full conditional distribution for M_k is given by

$$[M_k \mid \text{others}] \sim \text{Ga}(a_k, b_k)$$

where

$$a_k = a_{\gamma_k} + J_k,$$

$$b_k = b_{\gamma_k} + 1.$$

- Full conditional posterior of σ^2

$$\begin{aligned} [\sigma^2 \mid \text{others}, \mathbf{Y}] &\propto \left[(\sigma^2)^{-\frac{n}{2}} \times \exp \left\{ -\frac{1}{2\sigma^2} \sum_{i=1}^n (y_i - \beta_0 - \sum_{k \in S} \sum_{l=1}^{J_k} B_k(x; \boldsymbol{\xi}_{k,l}) \beta_{k,l})^2 \right\} \right] \\ &\times \left[(\sigma^2)^{-\frac{r}{2}+1} \times \exp \left\{ -\frac{rR}{2\sigma^2} \right\} \right] \\ &\propto (\sigma^2)^{-\frac{n+r}{2}+1} \exp \left\{ -\frac{1}{2\sigma^2} \sum_{i=1}^n (y_i - \beta_0 - \sum_{k \in S} \sum_{l=1}^{J_k} B_k(x; \boldsymbol{\xi}_{k,l}) \beta_{k,l})^2 - \frac{rR}{2\sigma^2} \right\} \end{aligned}$$

The full conditional distribution for σ^2 is

$$[\sigma^2 \mid \text{others}, \mathbf{Y}] \sim \text{IG} \left(\frac{r_0}{2}, \frac{r_0 R_0}{2} \right)$$

with

$$\begin{aligned} r_0 &= r + n, \\ R_0 &= \frac{\sum_{i=1}^n (y_i - \beta_0 - \sum_{k \in S} \sum_{l=1}^{J_k} B_k(x; \boldsymbol{\xi}_{k,l}) \beta_{k,l})^2 + rR}{r_0}. \end{aligned}$$